Molecular Pharmacology Fast Forward. Published on July 12, 2006 as doi: 10.1124/mol.106.026823

MOL 26823

1. Title page

Effects of potent inhibitors of the retinoid cycle on visual function and photoreceptor protection from light damage in mice

Akiko Maeda, Tadao Maeda, Marcin Golczak, Yoshikazu Imanishi, Patrick Leahy, Ryo Kubota, and Krzysztof Palczewski

Department of Pharmacology, Case School of Medicine, Case Western Reserve University, Cleveland, OH. (A.M., T.M., M.G., Y.I., K.P.);

Comprehensive Cancer Center, Case School of Medicine, Case Western Reserve University, Cleveland, OH. (P.L.);

Acucela Inc. Seattle, WA. (R.K.)

Molecular Pharmacology Fast Forward. Published on July 12, 2006 as DOI: 10.1124/mol.106.026823
This article has not been copyedited and formatted. The final version may differ from this version.

2. Running title page

a) *Running title*: Effects of retinylamine and its amides on vision.

b) Address Correspondence to:

Krzysztof Palczewski, Ph.D.

Department of Pharmacology

Case Western Reserve University

10900 Euclid Ave. BRB R924

Cleveland, Ohio 44106-4965, USA

Phone: 216-368-4631; Fax: 216-368-1300; E-mail: kxp65@case.edu

c) Number of text pages: 35

Number of tables: 2

Number of figures: 7

Number of references: 41

Number of words in the *Abstract*: 231

Number of words in the *Introduction*: 375

Number of words in the *Discussion*: 1043

Number of supplement tables: 2

Number of supplement figures: 5

d) Abbreviations: A2E, *N*-retinylidene-*N*-retinyl ethanolamine; CRALBP, cellular retinaldehyde-binding protein; CRBP, cellular retinoid-binding protein; ERG, electroretinogram; fenretinide, *N*-(4-hydroxyphenyl)retinamide; LRAT, lecithin:retinol

Molecular Pharmacology Fast Forward. Published on July 12, 2006 as DOI: 10.1124/mol.106.026823
This article has not been copyedited and formatted. The final version may differ from this version.

acyltransferase; OS, outer segment; RDH, retinol dehydrogenase; RPE, retinal pigment epithelium; Ret-NH_2, retinylamine; RPE65, an RPE-specific 65 kDa protein.

Molecular Pharmacology Fast Forward. Published on July 12, 2006 as DOI: 10.1124/mol.106.026823
This article has not been copyedited and formatted. The final version may differ from this version.

3. Abstract page

ABSTRACT

Regeneration of the chromophore, 11-*cis*-retinal, is essential for the generation of light-sensitive visual pigments in the vertebrate retina. A deficiency in 11-*cis*-retinal production leads to congenital blindness in humans; however, a buildup of the photoisomerized chromophore can also be detrimental. Such is the case when the photoisomerized all-*trans*-retinal is produced but cannot be efficiently cleared from the internal membrane of the outer segment discs. Sustained increase of all-*trans*-retinal can lead to the formation of toxic condensation products in the eye. Thus, there is a need for potent, selective inhibitors which can regulate the flux of retinoids through the metabolism pathway termed the visual (retinoid) cycle. Here we systematically study the effects of the most potent inhibitor of this cycle, retinylamine (Ret-NH_2), on visual function in mice. Prolonged, sustainable, but reversible suppression of the visual function was observed by Ret-NH_2 due to its storage in a pro-drug form, *N*-retinylamides. Direct comparison of other inhibitors such as fenretinide and 13-*cis*-retinoic acid showed multiple advantages of Ret-NH_2 and its amides, including a higher potency, specificity and lower transcription activation. Our results also revealed that mice treated with Ret-NH_2 were completely resistant to the light-induced retina damage. As an experimental tool, Ret-NH_2 allows the replacement of the native chromophore with synthetic analogs in wild-type mice to better understand the function of the chromophore in the activation of rhodopsin and its metabolism through the retinoid cycle.

Molecular Pharmacology Fast Forward. Published on July 12, 2006 as DOI: 10.1124/mol.106.026823
This article has not been copyedited and formatted. The final version may differ from this version.

4. Introduction page

INTRODUCTION

In the photoreceptors of the vertebrate retina, light causes the isomerization of the visual pigments' chromophore, 11-*cis*-retinylidene, to all-*trans*-retinylidene followed by the release of all-*trans*-retinal from the opsin binding pocket and its reduction to all-*trans*-retinol (Lamb and Pugh, 2004; McBee et al., 2001; Palczewski, 2006). Vitamin A (all-*trans*-retinol) diffuses to the retinal pigment epithelium (RPE) where it is esterified by lecithin:retinol acyltransferase (LRAT) to all-*trans*-retinyl esters and stored in the retinosomes (Imanishi et al., 2004a; Imanishi et al., 2004b). All-*trans*-retinyl esters are isomerized to 11-*cis*-retinol in a reaction that involves an abundant 65 kDa RPE-specific protein, termed RPE65, proposed to be retinoid isomerase (Jin et al., 2005; Moiseyev et al., 2005; Redmond et al., 2005). To complete the cycle, 11-*cis*-retinol is then oxidized to its aldehyde. 11-*cis*-Retinal diffuses across the extracellular space to photoreceptors and recombines with opsins to regenerate visual pigments (Lamb and Pugh, 2004; McBee et al., 2001).

The accumulation of fluorescent materials, lipofuscin, in the RPE is associated with aging. In humans, one of the major fluorescent compounds found most prominently in the macula is a pyridinium bis-retinoid, which is derived from two molecules of all-*trans*-retinal and one molecule of phosphatidylethanolamine, called A2E (Parish et al., 1998), which is toxic to the RPE cells. Extensive accumulation of A2E is observed in the recessive juvenile macular degeneration known as the Stargardt disease, caused by mutations in the human ABCR4 gene (Allikmets et al., 1997). ABCR4 is an ATP-binding cassette transporter that localizes to the outer segment (OS) disks of rods and cones

Molecular Pharmacology Fast Forward. Published on July 12, 2006 as DOI: 10.1124/mol.106.026823
This article has not been copyedited and formatted. The final version may differ from this version.

where it is thought to be involved in the transport of *N*-retinylidene-phosphatidylethanolamine (Beharry et al., 2004; Weng et al., 1999). Thus, properly functioning ABCR4 lowers all-*trans*-retinal and consequently decreases the probability of A2E adduct formation. Because it is unknown how to speed up the ABCR4 activity, another strategy proposed by Travis and colleagues was to reduce the flow of retinoids through the inhibition of the visual cycle and thus slow the production of the component of A2E, all-*trans*-retinal (Mata et al., 2000; Radu et al., 2003). The potential inhibitors of the visual cycle include 13-*cis*-retinoic acid (Accutane, Roche)(Radu et al., 2004a; Radu et al., 2003; Radu et al., 2004b), fenretinide (Radu et al., 2005), or various retinoids and farnesyl-containing isoprenoids (TDT and TDH), acting through interaction with RPE65 (Gollapalli and Rando, 2004). The phenotype observed with limited production of 11-*cis*-retinal includes delayed dark adaptation.

Visible light-induced photoreceptor cell damage results from the activation of rhodopsin and culminates in photoreceptor apoptosis. Mice lacking rhodopsin or lacking enzymes involved in the production of rhodopsin's chromophore are completely protected against light-induced apoptosis (Grimm et al., 2000). Prolonged inhibition of the chromophore production by 13-*cis*-retinoic acid protected rats from light damage (Sieving et al., 2001). Thus, inhibition of the visual cycle can be useful in some environmental conditions, and can be considered as a treatment of inherited and acquired retinal and macular degeneration.

Positively charged retinoids, all-*trans*-retinylamine (Ret-NH_2), and its isomers are potent inhibitors of the 11-*cis*-retinol isomerization in bovine RPE microsomes (Golczak et al., 2005b). The target for this inhibitor appears to be either a sub-fraction of RPE65, or

Molecular Pharmacology Fast Forward. Published on July 12, 2006 as DOI: 10.1124/mol.106.026823
This article has not been copyedited and formatted. The final version may differ from this version.

another protein essential for the isomerization reaction. We also found that Ret-NH_2 interacts only at micromolar concentrations with retinoic acid receptor and does not activate retinoid-X receptor (Golczak et al., 2005b). Moreover, the effect of this inhibitor was remarkably prolonged. This property has been attributed to the fact that Ret-NH_2 is reversibly *N*-acylated by LRAT to form inactive *N*-retinylamides (Golczak et al., 2005a). The presence of *N*-retinylamides was detected *in vivo* in wild-type mice supplemented with Ret-NH_2, but not in *lrat-/-* mice. *N*-Retinylamides are thus the main metabolites of Ret-NH_2 in the liver and the eye and can be mobilized back to Ret-NH_2 by hydrolysis. Mice treated with all-*trans*-Ret-NH_2 showed profound delayed dark adaptation following light exposure.

In this study, we further characterized the properties of all-*trans*-Ret-NH_2 *in vivo*. We asked how different doses of the inhibitor affect the metabolism of retinoids in the eye; how quickly is all-*trans*-Ret-NH_2 cleared from the eye and other organs; how the efficacy of all-*trans*-Ret-NH_2 compares to the efficacy of its amides and other known inhibitors of the visual cycle; and what are the genes that are activated by treatment with the inhibitor as a indicator of toxicity. We also questioned how all-*trans*-Ret-NH_2 can be employed as a research tool; and finally, how all-*trans*-Ret-NH_2 affects light-induced damage of photoreceptors.

Molecular Pharmacology Fast Forward. Published on July 12, 2006 as DOI: 10.1124/mol.106.026823
This article has not been copyedited and formatted. The final version may differ from this version.

5. Materials and Methods pages

MATERIALS AND METHODS

Animals — All animal experiments employed procedures approved by Case Western Reserve University, and conformed to recommendations of the American Veterinary Medical Association Panel on Euthanasia and recommendations of the Association of Research for Vision and Ophthalmology. Animals were maintained in complete darkness or on a 12 h light/12 h dark cycle, and all manipulations were done under dim red light employing a Kodak No. 1 safelight filter (transmittance >560 nm). Typically, 6-week-old female mice were used in all of the experiments. Animals were gavaged with Ret-NH_2 and other retinoids emulsified with 150 μl of vegetable oil as previously described (Van Hooser et al., 2000).

Chemical synthesis — Ret-NH_2 was prepared according to the published method (Golczak et al., 2005a). *N*-retinylacetamide and *N*-retinylpalmitamide were prepared by reacting Ret-NH_2 and an excess of acetic anhydride or palmitoyl chloride, respectively, in anhydrous dichloromethane in the presence of *N*,*N*-dimethylaminopyridine (DMAP) at 0 °C for 1 h. After the reaction was completed as judged by HPLC, water was added and the product was extracted with hexane. The hexane layer was washed with saturated NaCl solution, dried with anhydrous magnesium sulfate, filtered, and evaporated in a SpeedVac. Mass spectral analyses of synthesized retinoids were performed using a Kratos Analytical Instruments profile HV-3 direct probe mass spectrometer and electron-impact ionization. 13-*cis*-Retinoic acid and *N*-(4-hydroxyphenyl)retinamide (fenretinide) were purchased from Sigma or Toronto Research Chemicals Inc.

Molecular Pharmacology Fast Forward. Published on July 12, 2006 as DOI: 10.1124/mol.106.026823
This article has not been copyedited and formatted. The final version may differ from this version.

HPLC analysis of retinoids in the eye — All experimental procedures related to extraction, derivatization, and separation of retinoids from dissected mouse eyes were carried out under dim red light as previously described (Maeda et al., 2003). Retinoids were separated by normal phase HPLC (Ultrasphere-Si, 4.6 μ 250 mm, Beckman, Fullerton, CA) using 10% ethyl acetate and 90% hexane at a flow rate of 1.4 ml/min with detection at 325 nm employing an HP1100 HPLC with a diode array detector and HP Chemstation A.03.03 software.

HPLC Analysis of Ret-NH_2 and its amides in the liver and blood — Mouse tissues (two eyes, 0.5 g of liver or approximately 0.5 ml of blood) were homogenized and suspended in 3 ml of 20 mM bis-Tris-Propane (BTP), pH 7.4, containing 50% (v/v) of methanol. Retinoids were then extracted with 4 ml of hexane. The collected organic phase was evaporated using a SpeedVac, and the retinoids were redissolved in 400 μl of hexane. Typically 10 or 100 μl of the liver extract were injected on an HPLC column in order to detect *N*-retinylamides or Ret-NH_2, respectively. In the case of samples extracted from mouse eyes and blood, the same (100 μl) volume of retinoid solution was injected for *N*-retinylamides and Ret-NH_2 analysis. A normal phase column (Beckman Ultrasphere-Si, 5 μm, 4.5 x 250 mm) and a step gradient of ethyl acetate in hexane (10% ethyl acetate for 23 min and then 40% ethyl acetate up to 40 min) at a flow rate of 2 ml/min were used to elute *N*-retinylamides. To detect Ret-NH_2, retinoid separation was performed in 99.5% ethyl acetate containing 0.5% of 7 M ammonia dissolved in methanol.

Molecular Pharmacology Fast Forward. Published on July 12, 2006 as DOI: 10.1124/mol.106.026823
This article has not been copyedited and formatted. The final version may differ from this version.

Liver retinoic acid analysis —Retinoic acid analysis was carried out using previously described methods (Batten et al., 2005). Extracted retinoic acid was injected onto tandem normal phase HPLC columns. The first column was a Varian Microsorb Silica column (Varian, Palo Alto, CA, 3 μ, 4.6 × 100 mm), and the second was the Beckman column (Beckman Ultrasphere-Si, 5 μm, 4.5 x 250 mm). An isocratic solvent system of 1,000:4.3:0.675 hexane:2-propanol:glacial acetic acid (v/v) was used at a flow rate of 1 ml/min at 20 °C with detection at 355 nm calibrated using standards of all-*trans*-retinoic acid and 9-*cis*-retinoic acid purchased from Sigma-Aldrich.

Electroretinograms (ERGs) —ERG were recorded as previously reported (Maeda et al., 2005; Maeda et al., 2003). All experimental procedures were performed under safety light. Dark-adapted mice were anesthetized by intraperitoneal injection using 20 μl/g body weight of 6 mg/ml ketamine and 0.44 mg/ml xylazine diluted with 10 mM sodium phosphate, pH 7.2, containing 100 mM NaCl. The pupils were dilated with 0.01% tropicamide. A contact lens electrode was placed on the eye, and a reference electrode and ground electrode were placed in the ear and the tail. ERGs were recorded with the universal electrophysiologic system UTAS E-3000 (LKC Technologies, Inc.). The light intensity was calibrated by the manufacturer and was computer-controlled. The mice were placed in a Ganzfeld dome, and scotopic and photopic responses to flash stimuli were each obtained from both eyes simultaneously.

Induction and analysis of light damage — Light damage was induced as previously described (Wenzel et al., 2001) with some modifications. Before exposure to light, Balb/c

Molecular Pharmacology Fast Forward. Published on July 12, 2006 as DOI: 10.1124/mol.106.026823
This article has not been copyedited and formatted. The final version may differ from this version.

mice (female, 6-week-old) were dark-adapted for 48 h. Light damage was induced in mice without dilated pupils by exposure to 5,000 lux of diffuse white fluorescent light (150 W spiral lamp, Commercial Electric, USA) for 2 h (lights on at 11:00 A.M.). These mice were kept under dark conditions for 7 days and evaluated by ERG, histological study, and rhodopsin measurement.

Histological study — For light microscopy, mouse eyecups were fixed by immersion in 2.5% glutaraldehyde and 1.6% paraformaldehyde in 0.08 M PIPES, pH 7.4, containing 2% sucrose, at room temperature for ~1 h initially and then at 4 °C for 24 h. The eyecups were then washed with 0.13 M sodium phosphate, pH 7.3, dehydrated through a CH_3OH series, and embedded in JB4 glycol metacrylat. The sections (6 μm) were stained by immersion with 5% Richardson's stain for 1.5 - 2 min at room temperature, and de-stained in 0.13 M phosphate buffer for 8-15 min until the layers could be visualized under a microscope.

Rhodopsin measurements — Typically, two mouse eyes were used per rhodopsin measurement. Mouse eyes were enucleated and rinsed with water. The lenses were removed, and the eyes were cut into three or four pieces and frozen immediately on a dry ice/ethanol bath. Rhodopsin was extracted with 0.9 ml of 20 mM BTP, pH 7.5, containing 10 mM *n*-dodecyl-β-maltoside and 5 mM freshly neutralized NH_2OH-HCl. The sample was homogenized with a Dounce tissue homogenizer and shaken for 5 min at room temperature. The sample was then centrifuged at 14,000 rpm for 5 min at room temperature. The supernatant was collected, and the pellet was extracted one more time.

Molecular Pharmacology Fast Forward. Published on July 12, 2006 as DOI: 10.1124/mol.106.026823
This article has not been copyedited and formatted. The final version may differ from this version.

The combined supernatants were centrifuged at 50,000 rpm for 10 min, and absorption spectra were recorded before and after a 12 min bleach (60 W incandescent bulb). The concentration of rhodopsin was determined by the decrease in absorption at 500 nm using the molar extinction coefficient $\epsilon = 42{,}000\ M^{-1}\ cm^{-1}$.

Immunocytochemistry of arrestin and transducin α-subunit —Rabbit anti-arrestin polyclonal antibody was a generous gift from Dr. G. S. Wu (University of South California, Los Angeles). Mouse anti-transducin α-subunit monoclonal antibody was generated against a 12-amino acid long peptide corresponding to the C-terminal region of bovine transducin α-subunit coupled to Keyhole Limpet Hemocyanin (KLH) (K. Palczewski, and K. Ridge, University of Texas, Houston, unpublished). Retina sections were incubated in 1.5% normal goat serum in PBST buffer (136 mM NaCl, 11.4 mM sodium phosphate, 0.1% Triton X-100, pH 7.4) for 15 min at room temperature to block non-specific labeling, incubated with purified anti-arrestin or anti-transducin α-subunit antibody overnight at 4˚C, rinsed with PBST, incubated with indocarbocyanine (Cy3)-conjugated goat anti-mouse IgG or anti-rabit IgG, rinsed with PBST, mounted in 50 µl 2% 1,4-diazabicyclo-2,2,2-octane in 90% glycerol to retard photobleaching, and analyzed under a Leica DM6000 B microscope equipped with a RETIGA EXi CCD camera (Q-Imaging, BC, Canada).

Mouse treatment for the array analysis —Mice were dark adapted for 48 h, gavaged with either 2 µmol of 13-*cis*-retinoic acid, fenretinide, or Ret-NH_2, kept in the dark for 16 h after the gavage, and total RNA was isolated from 10 eyes or from 100 mg liver of each

Molecular Pharmacology Fast Forward. Published on July 12, 2006 as DOI: 10.1124/mol.106.026823
This article has not been copyedited and formatted. The final version may differ from this version.

group with a RiboPure™ Kit (Ambion). The quality of the RNA was verified by RNA agarose gel electrophoresis and using the Agilent Bioanalyzer. Aliquots of total RNA isolated from the different tissues and from mice undergoing the various treatments were detection-labeled and hybridized on the mouse genomic microarray using a service provided by NimbleGen System Inc. Services (Madison, WI). The microarray contained the 37,364 genes and covered the entire mouse transcriptome as represented by the University of California, Santa Cruz database (build HG 17), using a minimum of 11 probes per gene. The expression of genes was normalized according to probe signal and the average signal for each gene was normalized for each sample replicate.

Array data for samples across the whole study were normalized by NimbleGen Systems Inc., using the RMA (robust multichip analysis) feature of the data analysis package contained in www.bioconductor.org. Project-wide spread-sheets of RMA results were exported to Microsoft Excel and expression level ratios for all possible pair-wise comparisons, comprising one control and one treated sample, were calculated. These pair-wise ratios were imported to Microsoft Access and mined for credible fold changes. Changes in gene expression greater than or equal to 2 fold for increases or less than or equal to 0.5 fold for decreases were considered significant. The differentially expressed genes were then exported from Access as Excel files and were annotated using Lucidyx Searcher software (www.Lucidyx.com).

Molecular Pharmacology Fast Forward. Published on July 12, 2006 as DOI: 10.1124/mol.106.026823
This article has not been copyedited and formatted. The final version may differ from this version.

6. Results pages

RESULTS

Effects of Ret-NH_2 on retinoid metabolism in the eye, blood, and liver — First, we tested the recovery of 11-*cis*-retinal and the accumulation of esters in the mouse eyes after a treatment with all-*trans*-Ret-NH_2. A wide range of the inhibitor, from 1.75 to 17.5 μmol/treatment, suppressed recovery of more than 80% of the 11-*cis*-retinal level when treated mice were exposed to light (Figure 1A). Because there are no significant amounts of free 11-*cis*-retinal in the mouse eye, 11-*cis*-retinal is equivalent to the rhodopsin level (Palczewski et al., 1999). In untreated mice the recovery of full dark adaptation was observed in 24 h (*Inset*, Figure 1A), while upon Ret-NH_2 administration it was slower, reaching 50% of the normal 11-*cis*-retinal level in about 3 days for lower doses and about 10 days for the 17.5 μM dose. The highest dose suppressed 11-*cis*-retinal production for as long as 7 days of dark adaptation before recovery was observed (Figure 1A). To test the suppression of the isomerization reaction during the recovery phase, mice that were treated with 3.5 μmol of the inhibitor and exposed to light after 7 days were examined for recovery of visual chromophore. Under these conditions, during the first 5 h of dark adaptation only 20% of 11-*cis*-retinal was recovered in treated mice while 80% was recovered in control mice (*Inset*, Figure 1A). These results suggest that the isomerization is still significantly inhibited after 7 days, but because the mice were kept in the dark, 11-*cis*-retinal, albeit produced at a slower rate, was trapped by opsin which contributed to the observed recovery of the chromophore in these mice.

Second, the all-*trans*-retinyl ester level was elevated in the Ret-NH_2-treated mice proportional to the level of the isomerized chromophore in the eye. Possible

Molecular Pharmacology Fast Forward. Published on July 12, 2006 as DOI: 10.1124/mol.106.026823
This article has not been copyedited and formatted. The final version may differ from this version.

transformations involved isomerization of 11-*cis*-retinal to all-*trans*-retinal, reduced to all-*trans*-retinol, and esterified to form all-*trans*-retinyl esters (Figure 1B). Conversely, the reduction of the ester levels was proportional to the recovery of 11-*cis*-retinal. Although Ret-NH_2 can be converted to all-*trans*-retinol and subsequently to all-*trans*-retinyl esters (Golczak et al., 2005a), the ester analysis suggested that the ester accumulation cannot be attributed to deaminated and esterified Ret-NH_2.

Third, the clearance of Ret-NH_2 and retinylamide after a single dose varying from 1.75 to 17.5 μmol of Ret-NH_2 was measured in the liver, blood, and eye samples (Figure 2). The level of Ret-NH_2 spiked in 2 h after gavage in all three tissues analyzed and remained stable at low levels throughout the experiment. In the liver, the amide peaked in 3-5 days (Figure 2). In the eye, faster intake and decay of the amides was observed, while in the blood a spike was only observed 2 h after gavage (Figure 2). Storage of Ret-NH_2 in the liver and eye facilitates the prolonged effect of this inhibitor in blocking the visual function. Similar results were obtained when mice were treated with *N*-retinylacetamide.

Comparison of the effect of *N*-retinylacetamide, *N*-retinylpalmitamide, Ret-NH_2, and other inhibitors on the retinoid cycle — To compare the potency of two other inhibitors of the visual cycle *N*-(4-hydroxyphenyl)retinamide (4-HPR or fenretinide) and 13-*cis*-retinoic acid (Accutane) side-by–side with Ret-NH_2, *N*-retinylpalmitamide and *N*-retinylacetamide, mice were gavaged with one of the three select doses of inhibitors, exposed to light, and analyzed 5 h and 24 h later after dark adaptation (Figure 3). For fenretinide and 13-*cis*-retinoic acid only the highest dose was employed. After 5 h, a significant inhibition was observed for Ret-NH_2 > *N*-retinylpalmitamide = *N*-

Molecular Pharmacology Fast Forward. Published on July 12, 2006 as DOI: 10.1124/mol.106.026823
This article has not been copyedited and formatted. The final version may differ from this version.

retinylacetamide, after 24 h of dark adaptation, the inhibition was observed only for Ret-NH_2. The analysis of free Ret-NH_2 indicated that the amine was generated from the amide and the level of the amine decreased with time of dark adaptation and remained only at significant levels for the highest dose (Figure 3). This observation correlates well with the significant inhibition under these conditions. These results suggest that Ret-NH_2 is the most potent among all tested inhibitors, implying that the lowest dose will be required to achieve a therapeutic effect as compared with other inhibitors, and that the inhibition by Ret-NH_2 has a long-lasting effect. Indeed, the regeneration was suppressed in a dose dependent manner (Figure 3). The lower absorption of *N*-retinylamides was observed compared with Ret-NH_2 (unpublished data), explaining the significantly reduced efficacy of the amidated form of the inhibitor.

To measure how quickly *N*-retinylacetamide becomes effective in the inhibition of the visual cycle after treatment, mice were exposed to illumination that bleached about 50% of rhodopsin. After 2 h of treatment, no inhibition was apparent, but after 4 h and 8 h, suppression of 11-*cis*-retinal production was observed (Figure S1). A longer period of dark adaptation, about 16 h, reduced the effectiveness of the drug, likely due to its being catabolized. As little as 1.75-3.5 μmol of *N*-retinylacetamide was sufficient to completely suppress the regeneration reactions in our standard conditions (Figure S2), which was similar to the quantities for Ret-NH_2.

Potential side effects on the visual cycle inhibtors — A series of experiments was carried out to assess the potential side effects of Ret-NH_2 in mice. Four treatments with 7 day-intervals produced elevated esters 7 days after the last gavage and, as expected,

Molecular Pharmacology Fast Forward. Published on July 12, 2006 as DOI: 10.1124/mol.106.026823
This article has not been copyedited and formatted. The final version may differ from this version.

suppressed 11-*cis*-retinal levels, but 2 months after the last gavage the composition of retinoids was normal (Figure S3A). The a-waves and b-waves of the ERG were slightly suppressed in scotopic conditions and significantly suppressed in photopic conditions at high light intensities 7 days after the last gavage, but recovered completely two months later (Figure S3B). Finally, the body weights of multiple treated mice were unchanged compared with the control mice (Figure S3C). We further examined a maintenance dose of Ret-NH_2 which can completely suppress 11-*cis*-retinal production for a long period in dark conditions. When light exposure (~90% rhodopsin bleach) was performed 4 h after the gavage, gavage of 3.5 μmol Ret-NH_2 every other day continued inhibiting 11-*cis*-retinal production, whereas a gradual increase of 11-*cis*-retinal was observed in the mice treated with 1.75 μmol Ret-NH_2 (Figure S4), suggesting that long term complete blockage of 11-*cis*-retinal production can be maintained by multiple gavages of 3.5 μmol of Ret-NH_2.

Ret-NH_2 can be oxidized through retinol, and retinal into retinoic acid. Thus, next, we tested the levels of all-*trans*-retinoic acid after the treatment with Ret-NH_2 in mice. Compared with retinol treatment, only a trace elevation of potentially toxic all-*trans*-retinoic acid was detected (Table 1), suggesting that the metabolism of Ret-NH_2 in mice does not lead to elevated formation/accumulation of the ligand for the nuclear hormone receptors.

Retinoic acids are activators of nuclear hormone receptors (Chambon, 1996). Our previous study demonstrated that Ret-NH_2 do not efficiently activate the RAR or RXR nuclear hormone receptors *in vitro* (Golczak et al., 2005b). However, that are number of nuclear receptors for which the ligand were not identified, and the *in vitro* study carries

Molecular Pharmacology Fast Forward. Published on July 12, 2006 as DOI: 10.1124/mol.106.026823
This article has not been copyedited and formatted. The final version may differ from this version.

obvious risk of over-interpretation. Thus, the expression levels of mRNA were compared between mice treated with 13-*cis*-retinoic acid, fenretinide, and Ret-NH_2 using a 37,364 gene array provided by NimbleGen System Inc. (Madison, WI). In the liver, 13-*cis*-retinoic acid caused elevated expression, by a factor of 2 or more, of more than 700 genes, as the two other inhibitors produced increases in 345 genes for fenretinide and 367 genes for Ret-NH_2, respectively (Figure 4). In the liver, 13-*cis*-retinoic acid caused suppression of the expression of more than 3,000 genes, and the two other inhibitors decreased expression of 322 genes for fenretinide and 230 genes for Ret-NH_2, respectively (Figure 4). In the eye, the gene expression pattern was less dramatically changed for 13-*cis*-retinoic acid, while fenretinide and Ret-NH_2 had comparable effects as in the liver (Figure 4). The specific genes whose expressions were the most affected are listed in Tables 1S and 2S of the supplement. In the eye, the increased γ-crystallin protein level was also demonstrated by immunoblotting (Figure S5). A wide range of proteins/enzymes were identified, but not one group of enzymes involved in one specific pathway or transformation appears to be obvious from the analysis. Instead, as exprected, a global misregulation of gene expression was observed mostly for 13-*cis*-retinoic acid, while Ret-NH_2 and fenretinide had less of an effect on the gene expression. For these two last inhibitors, the pattern of gene expression was similar. Thus, Ret-NH_2 leads to the least amount of altered gene expression patterns compared to other proposed visual cycle inhibitors.

Deficiencies of arrestin and transducin α-subunit translocation in Ret-NH_2 administrated mice — Light-dependent movement of photoreceptor proteins is an

Molecular Pharmacology Fast Forward. Published on July 12, 2006 as DOI: 10.1124/mol.106.026823
This article has not been copyedited and formatted. The final version may differ from this version.

essential mechanism of photoreceptor adaptation to the ambient light levels (Sokolov et al., 2002), and could be used to assess the functionality of the phototransduction when the inhibitor is employed. Mice treated with Ret-NH_2 showed partial reduction in light-dependent arrestin and rod photoreceptor G protein, transducin, α-subunit translocations. In mice treated with Ret-NH_2, arrestin was localized throughout the photoreceptor cells independent of light conditions (Figure 5A, right). Slight translocation of arrestin to OS was observed by light adaptation (Figure 5A, bottom right) suggesting functional rhodopsin molecules remained at low levels in Ret-NH_2-treated animals. Reduction in transducin movement was also observed in Ret-NH_2-treated mice (Figure 5B). In the light adapted retina, OS still retained substantial amounts of transducin α-subunit (Figure 5B, bottom right). These results indicate that Ret-NH_2 treatment causes deficiency in the light adaptation of rod photoreceptors, most likely by depleting rhodopsin's chromophore.

Substitution of 11-*cis*-retinal by 9-*cis*-retinal during the suppression of the visual cycle — During suppression of the regeneration pathway by Ret-NH_2, the visual pigment can be rescued by the exogenous chromophore 9-*cis*-retinal (Figure 6A). Two doses of Ret-NH_2 were tested as shown in Figure 6A. Two days after 9-*cis*-retinyl acetate gavage, scotopic and photopic ERGs showed significant improvements (Figure 6B). Interestingly, when mice were kept in darkness after regeneration, 9-*cis*-retinal was consequently replaced by naturally produced 11-*cis*-retinal after about two weeks; thus in a time course needed for complete renewal of the photoreceptor by phagocytosis (Figure 6A). These observations suggest that rhodopsin is more stable with 11-*cis*-retinal or that opsin has higher affinity for 11-*cis*-retinal as observed experimentally (Kandori et al., 1988; Lacy et

Molecular Pharmacology Fast Forward. Published on July 12, 2006 as DOI: 10.1124/mol.106.026823
This article has not been copyedited and formatted. The final version may differ from this version.

al., 1984). This experiment also demonstrates that Ret-NH_2 does not directly affect re-coupling of the chromophore with the opsin.

The protective effect of Ret-NH_2 on light-induced retinal damage in mice — Mice lacking the active chromophore 11-*cis*-retinal or rhodopsin, *rpe65-/-* and *rho-/-* mice, are resistant to light damage (Grimm et al., 2000). These observations suggest that rhodopsin is responsible for light-induced photoreceptor degeneration (Grimm et al., 2000). Five lines of histological, biochemical and electrophysiological data support the idea that Ret-NH_2 prevents light-induced damage to the eye. First, the histological sections showed that the retinas of the Ret-NH_2-treated mice have fully preserved photoreceptor layers (Figure 7A), compared with mice not exposed to light. Second, the amount of 11-*cis*-retinal decreased dramatically in mice exposed to light but not among those gavaged with Ret-NH_2 after sufficient dark adaptation (Figure 7B). Third, rhodopsin levels were considerably diminished to about 20% of the control levels. This was not observed when mice were treated with the isomerase inhibitor (Figure 7C, Table 2). Fourth, immunoblots from mice treated with Ret-NH_2 and exposed to strong illumination showed impressive preservation of rhodopsin (Figure 7D). Fifth, scotopic and photopic ERG showed preservation of rod- and cone-mediated vision as measured by the a-wave and b-wave amplitudes under different light intensities (Figure 7D-H). Thus, reversible inhibition of the retinoid cycle is an effective way to protect vision from damage caused by intense light.

Molecular Pharmacology Fast Forward. Published on July 12, 2006 as DOI: 10.1124/mol.106.026823
This article has not been copyedited and formatted. The final version may differ from this version.

7. Discussion pages

DISCUSSION

Dose dependent, prolonged, sustainable, and reversible suppression of the visual function by Ret-NH_2 — Ret-NH_2 is a potent inhibitor of the visual cycle (Golczak et al., 2005a; Golczak et al., 2005b; Maeda et al., 2006), with a prolonged mode of action due to its reversible amidation. Thus, the suppression of the visual function depends on the level of the accumulated amides of Ret-NH_2 (Figure 2). A single dose of the inhibitor (17.5 μmol) affects production for 11-*cis*-retinal for as long as 8 days (Figure 1). Bleaching of the visual pigments and conversion of 11-*cis*-retinal to all-*trans*-retinal and subsequently to all-*trans*-retinol led to transient accumulation of all-*trans*-retinyl esters as the retinol formed was quickly esterified (Figure 1). This blockage in the 11-*cis*-retinal production is reversible because the inhibitor is metabolized to all-*trans*-retinol (Golczak et al., 2005a) and/or secreted (Figure 2).

No adverse affects were observed during husbandry for multiple gavaged mice for several parameters including the retinoid content in the eye, visual responses, or body weight (Figure S4). With a proper dose, the 11-*cis*-retinal production could be suppressed for as long as 7 days, the longest period studied here (Figure S4). The metabolism of the inhibitor to retinol is one of the most important toxicological safety features that set it apart from other inhibitors of the visual cycle.

The visual function was mostly investigated by ERG, by regeneration of rhodopsin, and by studying the light-dependent movement of two rod photoreceptor proteins after treatment with the inhibitor. Arrestin and transducin α-subunit are the two most abundant soluble photoreceptor proteins showing massive light-dependent

Molecular Pharmacology Fast Forward. Published on July 12, 2006 as DOI: 10.1124/mol.106.026823
This article has not been copyedited and formatted. The final version may differ from this version.

translocation. In the dark-adapted retina, arrestin is localized mostly throughout the photoreceptor cells (Figure 5A top left), and the transducin α-subunit is observed specifically in OS (Figure 5B top left). Upon photoactivation of rhodopsin and light adaptation of photoreceptors, arrestin relocates to OS (Figure 5A bottom left), and transducin α-subunits move out of the OS (Figure 5B bottom left). These results are consistent with the light-dependent translocation of those proteins analyzed by immunoblotting and immunocytochemistry (Sokolov et al., 2002). Currently, two processes are considered to trigger arrestin translocation to OS: 1) passive diffusion and arrestin-rhodopsin interaction; and 2) the phototransduction cascade mediated by transducin (Strissel et al., 2006). Although these two possible triggers are distinct, both require rhodopsin. In mice treated with Ret-NH_2, and depleted by photobleaching, no significant movement was observed. These results are consistent with the lack of translocation of arrestin in mice lacking the chromophore due to disruption of the RPE65 gene (Mendez et al., 2003).

Opsin versus isorhodopsin versus rhodopsin — Treatment of wild-type mice with Ret-NH_2 paves the way to study visual processes in genetically unmodified mice. The effect of opsin on the cell biology of signal transduction is easily accessible in a precise manner. Detailed studies of the phototransduction became achievable in rod photoreceptors containing different ratios of opsin to rhodopsin. Finally, replacement of the chromophore will allow us to follow the flow, e.g. the isotope-labeled synthetic chromophore, and to investigate how the chromophore modifications affect rhodopsin regeneration (e.g. see Figure 6). Regeneration of opsin by artificial chromophores would also allow tracking of

Molecular Pharmacology Fast Forward. Published on July 12, 2006 as DOI: 10.1124/mol.106.026823
This article has not been copyedited and formatted. The final version may differ from this version.

the integrity and maintenance of photoreceptor OSs by a non-invasive spectroscopic approach. Thus, Ret-NH_2 is a promising research tool to study the visual cycle and phototransduction.

Direct comparison of Ret-NH_2, its amides, fenretinide, and 13-*cis*-retinoic acid — Ret-NH_2 appears to be the most potent inhibitor (Golczak et al., 2005b), however, a large proportion of Ret-NH_2 is amidated and inactive in blocking the visual cycle (Figure 3). Amides are also less efficiently absorbed further lowering their effective dose. In the condition employed, Ret-NH_2 displayed significant levels of inhibition, while at the same molar dose no inhibition of 11-*cis*-retinal regeneration was observed by fenretinide and 13-*cis*-retinoic acid. Thus, Ret-NH_2 is a much more effective inhibitor compared with these other retinoid inhibitors *in vivo*. When we compared the effects of the expression of eye and liver genes induced by these inhibitors, the strongest activation/inhibition of gene expression was induced by 13-*cis*-retinoic acid, while fenretinide and Ret-NH_2 were less active. Taking into account the dose-dependent potency of the inhibition and the longer retention *in vivo*, Ret-NH_2 has a better safety profile than these other inhibitors.

Complete protection from the light damage —In some conditions, light-induced apoptosis of photoreceptors (Joseph and Li, 1996; Lansel et al., 1998; Organisciak et al., 1998) is triggered by rhodopsin (Grimm et al., 2000). Photoreceptors lacking opsin or rhodopsin are completely protected against light-induced apoptosis, suggesting that rhodopsin is essential for the intracellular death signal induced by light (Grimm et al., 2000). This previous observation is consistent with light damage observed in wild-type

Molecular Pharmacology Fast Forward. Published on July 12, 2006 as DOI: 10.1124/mol.106.026823
This article has not been copyedited and formatted. The final version may differ from this version.

mice employed in the current study. Inhibition of the chromophore production using Ret-NH_2 in genetically unaltered mice resulted in complete resistance against light-induced photoreceptor damage (Figure 7; Table 2).

Light damage occurs by at least two distinct pathway (Jacobson and McInnes, 2002), both initiated by rhodopsin. Mice lacking rhodopsin or proteins involved in production of the visual chromophore are resistant to light damage (Grimm et al., 2000). Ret-NH_2 inhibits 11-*cis*-retinal production, resulting in reduction of the amount of rhodopsin that can be activated by light, protecting retinal cells from light damage. One of the potential side effects is delay dark adaptation, which should not be equated with night blindness, because the treated mice recover the visual pigment rhodopsin, albeit slower (Figure 1).

Potential application to treat human eye diseases — The most exciting aspect of the study is the potential application of Ret-NH_2 for treatment of A2E-accumulating ocular diseases. Accumulation of A2E, which is toxic for the RPE, has been proposed to be an etiologic factor not only for Stargardt disease (Mata et al., 2001; Mata et al., 2000; Weng et al., 1999), but also for age-related macular degenerations (Mata et al., 2000). Inhibiting A2E formation should therefore slow the progression of visual loss in diseases associated with A2E over-accumulation. Thus, the current study is an important prelude for understanding the metabolism, the proper doses, timing, and mechanism of the drug action. Critically important is the reversibility of the visual suppression and restoration of normal retinoid content after treatment. Ret-NH_2 can also be applied to prevent the light-mediated retina damage (e.g., extensive light exposure from endoillumination sources

Molecular Pharmacology Fast Forward. Published on July 12, 2006 as DOI: 10.1124/mol.106.026823
This article has not been copyedited and formatted. The final version may differ from this version.

during prolonged retina surgery).

Molecular Pharmacology Fast Forward. Published on July 12, 2006 as DOI: 10.1124/mol.106.026823
This article has not been copyedited and formatted. The final version may differ from this version.

8. Acknowledgements page

ACKNOWLEDGEMENTS

We would like to thank Dr. A. R. Moise for help with the gene array experiments, and Melissa Puffenbarger for help with manuscript preparation. We thank Drs. N. Rao and G. S. Wu and for providing the arrestin antibody, and Drs R. Tzekov and A. R. Moise for the comments on the manuscript. University of Washington and Acucela Inc. may commercialize some of the technology described in this work. KP is a consultant for Acucela Inc.

Molecular Pharmacology Fast Forward. Published on July 12, 2006 as DOI: 10.1124/mol.106.026823
This article has not been copyedited and formatted. The final version may differ from this version.

9. References pages

REFERENCES

Allikmets R, Singh N, Sun H, Shroyer NF, Hutchinson A, Chidambaram A, Gerrard B, Baird L, Stauffer D, Peiffer A, Rattner A, Smallwood P, Li Y, Anderson KL, Lewis RA, Nathans J, Leppert M, Dean M and Lupski JR (1997) A photoreceptor cell-specific ATP-binding transporter gene (ABCR) is mutated in recessive Stargardt macular dystrophy. *Nat Genet* **15**:236-246.

Batten ML, Imanishi Y, Tu DC, Doan T, Zhu L, Pang J, Glushakova L, Moise AR, Baehr W, Van Gelder RN, Hauswirth WW, Rieke F and Palczewski K (2005) Pharmacological and rAAV Gene Therapy Rescue of Visual Functions in a Blind Mouse Model of Leber Congenital Amaurosis. *PLoS Med* **2**:e333.

Beharry S, Zhong M and Molday RS (2004) N-retinylidene-phosphatidylethanolamine is the preferred retinoid substrate for the photoreceptor-specific ABC transporter ABCA4 (ABCR). *J Biol Chem* **279**:53972-53979.

Chambon P (1996) A decade of molecular biology of retinoic acid receptors. *Faseb J* **10**:940-954.

Golczak M, Imanishi Y, Kuksa V, Maeda T, Kubota R and Palczewski K (2005a) Lecithin:retinol acyltransferase is responsible for amidation of retinylamine, a potent inhibitor of the retinoid cycle. *J Biol Chem* **280**:42263-42273.

Golczak M, Kuksa V, Maeda T, Moise AR and Palczewski K (2005b) Positively charged retinoids are potent and selective inhibitors of the trans-cis isomerization in the retinoid (visual) cycle. *Proc Natl Acad Sci U S A* **102**:8162-8167.

Gollapalli DR and Rando RR (2004) The specific binding of retinoic acid to RPE65 and approaches to the treatment of macular degeneration. *Proc Natl Acad Sci U S A* **101**:10030-10035.

Grimm C, Wenzel A, Hafezi F, Yu S, Redmond TM and Reme CE (2000) Protection of Rpe65-deficient mice identifies rhodopsin as a mediator of light-induced retinal degeneration. *Nat Genet* **25**:63-66.

Imanishi Y, Batten ML, Piston DW, Baehr W and Palczewski K (2004a) Noninvasive two-photon imaging reveals retinyl ester storage structures in the eye. *J Cell Biol* **164**:373-383.

Imanishi Y, Gerke V and Palczewski K (2004b) Retinosomes: new insights into intracellular managing of hydrophobic substances in lipid bodies. *J Cell Biol* **166**:447-453.

Jacobson SG and McInnes RR (2002) Blinded by the light. *Nat Genet* **32**:215-216.

Jin M, Li S, Moghrabi WN, Sun H and Travis GH (2005) Rpe65 is the retinoid isomerase in bovine retinal pigment epithelium. *Cell* **122**:449-459.

Joseph RM and Li T (1996) Overexpression of Bcl-2 or Bcl-XL transgenes and photoreceptor degeneration. *Invest Ophthalmol Vis Sci* **37**:2434-2446.

Kandori H, Matuoka S, Nagai H, Shichida Y and Yoshizawa T (1988) Dependency of apparent relative quantum yield of isorhodopsin to rhodopsin on the photon density of picosecond laser pulse. *Photochem Photobiol* **48**:93-97.

Lacy ME, Veronee CD and Crouch RK (1984) Regeneration of rhodopsin and isorhodopsin in rod outer segment preparations: absence of effect of solvent parameters. *Physiol Chem Phys Med NMR* **16**:275-281.

Lamb TD and Pugh EN, Jr. (2004) Dark adaptation and the retinoid cycle of vision. *Prog Retin Eye Res* **23**:307-380.

Lansel N, Hafezi F, Marti A, Hegi M, Reme C and Niemeyer G (1998) The mouse ERG before and after light damage is independent of p53. *Doc Ophthalmol* **96**:311-320.

Maeda A, Maeda T, Imanishi Y, Golczak M, Moise AR and Palczewski K (2006) Aberrant metabolites in mouse models of congenital blinding diseases: formation and storage of retinyl esters. *Biochemistry* **45**:4210-4219.

Maeda A, Maeda T, Imanishi Y, Kuksa V, Alekseev A, Bronson JD, Zhang H, Zhu L, Sun W, Saperstein DA, Rieke F, Baehr W and Palczewski K (2005) Role of photoreceptor-specific retinol dehydrogenase in the retinoid cycle in vivo. *J Biol Chem* **280**:18822-18832.

Maeda T, Van Hooser JP, Driessen CA, Filipek S, Janssen JJ and Palczewski K (2003) Evaluation of the role of the retinal G protein-coupled receptor (RGR) in the vertebrate retina in vivo. *J Neurochem* **85**:944-956.

Mata NL, Radu RA, Clemmons RC and Travis GH (2002) Isomerization and oxidation of vitamin a in cone-dominant retinas: a novel pathway for visual-pigment regeneration in daylight. *Neuron* **36**:69-80.

Mata NL, Ruiz A, Radu RA, Bui TV and Travis GH (2005) Chicken Retinas Contain a Retinoid Isomerase Activity that Catalyzes the Direct Conversion of all-trans-Retinol to 11-cis-Retinol. *Biochemistry* **44**:11715-11721.

Mata NL, Tzekov RT, Liu X, Weng J, Birch DG and Travis GH (2001) Delayed dark-adaptation and lipofuscin accumulation in abcr+/- mice: implications for involvement of ABCR in age-related macular degeneration. *Invest Ophthalmol Vis Sci* **42**:1685-1690.

Mata NL, Weng J and Travis GH (2000) Biosynthesis of a major lipofuscin fluorophore in mice and humans with ABCR-mediated retinal and macular degeneration. *Proc Natl Acad Sci U S A* **97**:7154-7159.

McBee JK, Palczewski K, Baehr W and Pepperberg DR (2001) Confronting complexity: the interlink of phototransduction and retinoid metabolism in the vertebrate retina. *Prog Retin Eye Res* **20**:469-529.

Mendez A, Lem J, Simon M and Chen J (2003) Light-dependent translocation of arrestin in the absence of rhodopsin phosphorylation and transducin signaling. *J Neurosci* **23**:3124-3129.

Moiseyev G, Chen Y, Takahashi Y, Wu BX and Ma JX (2005) RPE65 is the isomerohydrolase in the retinoid visual cycle. *Proc Natl Acad Sci U S A* **102**:12413-12418.

Organisciak DT, Darrow RM, Barsalou L, Darrow RA, Kutty RK, Kutty G and Wiggert B (1998) Light history and age-related changes in retinal light damage. *Invest Ophthalmol Vis Sci* **39**:1107-1116.

Palczewski K (2006) G protein-coupled receptor rhodopsin. *Annu Rev Biochem* **75**:743-767.

Palczewski K, Van Hooser JP, Garwin GG, Chen J, Liou GI and Saari JC (1999) Kinetics of visual pigment regeneration in excised mouse eyes and in mice with a targeted

disruption of the gene encoding interphotoreceptor retinoid-binding protein or arrestin. *Biochemistry* **38**:12012-12019.

Parish CA, Hashimoto M, Nakanishi K, Dillon J and Sparrow J (1998) Isolation and one-step preparation of A2E and iso-A2E, fluorophores from human retinal pigment epithelium. *Proc Natl Acad Sci U S A* **95**:14609-14613.

Radu RA, Han Y, Bui TV, Nusinowitz S, Bok D, Lichter J, Widder K, Travis GH and Mata NL (2005) Reductions in serum vitamin A arrest accumulation of toxic retinal fluorophores: a potential therapy for treatment of lipofuscin-based retinal diseases. *Invest Ophthalmol Vis Sci* **46**:4393-4401.

Radu RA, Mata NL, Bagla A and Travis GH (2004a) Light exposure stimulates formation of A2E oxiranes in a mouse model of Stargardt's macular degeneration. *Proc Natl Acad Sci U S A* **101**:5928-5933.

Radu RA, Mata NL, Nusinowitz S, Liu X, Sieving PA and Travis GH (2003) Treatment with isotretinoin inhibits lipofuscin accumulation in a mouse model of recessive Stargardt's macular degeneration. *Proc Natl Acad Sci U S A* **100**:4742-4747.

Radu RA, Mata NL, Nusinowitz S, Liu X and Travis GH (2004b) Isotretinoin treatment inhibits lipofuscin accumulation in a mouse model of recessive Stargardt's macular degeneration. *Novartis Found Symp* **255**:51-63; discussion 63-57, 177-178.

Redmond TM, Poliakov E, Yu S, Tsai JY, Lu Z and Gentleman S (2005) Mutation of key residues of RPE65 abolishes its enzymatic role as isomerohydrolase in the visual cycle. *Proc Natl Acad Sci U S A* **102**:13658-13663.

Sieving PA, Chaudhry P, Kondo M, Provenzano M, Wu D, Carlson TJ, Bush RA and Thompson DA (2001) Inhibition of the visual cycle in vivo by 13-cis retinoic acid protects from light damage and provides a mechanism for night blindness in isotretinoin therapy. *Proc Natl Acad Sci U S A* **98**:1835-1840.

Sokolov M, Lyubarsky AL, Strissel KJ, Savchenko AB, Govardovskii VI, Pugh EN, Jr. and Arshavsky VY (2002) Massive light-driven translocation of transducin between the two major compartments of rod cells: a novel mechanism of light adaptation. *Neuron* **34**:95-106.

Strissel KJ, Sokolov M, Trieu LH and Arshavsky VY (2006) Arrestin translocation is induced at a critical threshold of visual signaling and is superstoichiometric to bleached rhodopsin. *J Neurosci* **26**:1146-1153.

Van Hooser JP, Aleman TS, He YG, Cideciyan AV, Kuksa V, Pittler SJ, Stone EM, Jacobson SG and Palczewski K (2000) Rapid restoration of visual pigment and function with oral retinoid in a mouse model of childhood blindness. *Proc Natl Acad Sci U S A* **97**:8623-8628.

Weng J, Mata NL, Azarian SM, Tzekov RT, Birch DG and Travis GH (1999) Insights into the function of Rim protein in photoreceptors and etiology of Stargardt's disease from the phenotype in abcr knockout mice. *Cell* **98**:13-23.

Wenzel A, Reme CE, Williams TP, Hafezi F and Grimm C (2001) The Rpe65 Leu450Met variation increases retinal resistance against light-induced degeneration by slowing rhodopsin regeneration. *J Neurosci* **21**:53-58.

Molecular Pharmacology Fast Forward. Published on July 12, 2006 as DOI: 10.1124/mol.106.026823
This article has not been copyedited and formatted. The final version may differ from this version.

10. Foodnote page

This research was supported by NIH grant EY09339 and P30 EY11373, and a grant from National Neurovision Research Institute (AM). This research was supported by the Gene Expression and Genotyping Facility of the Comprehensive Cancer Center of Case Western Reserve University and University Hospitals of Cleveland (P30 CA43703).

Molecular Pharmacology Fast Forward. Published on July 12, 2006 as DOI: 10.1124/mol.106.026823
This article has not been copyedited and formatted. The final version may differ from this version.

11. Legends of Figure pages

FIGURE LEGENDS

Figure 1. Effects of different doses of Ret-NH_2 on the 11-*cis*-retinal and all-*trans*-retinyl ester levels in the eye. The 48 h dark-adapted C57BL/6 mice were gavaged with a single dose of Ret-NH_2 (1.75, 3.5, or 17.5 μmol). Next, 24 h after gavage, the mice were exposed to background light at 150 $cd \cdot m^{-2}$ for 20 min. Retinoid levels, 11-*cis*-retinal (A) and all-*trans*-retinyl ester (B), in the eye were examined at various times of dark adaptation. Retinoids were analyzed using HPLC methods as described in Materials and Methods. *Inset*, subset of mice gavaged with 3.5 μmol Ret-NH_2 were exposed a second time to the same intensity of illumination 7 days after the first exposure to light. All procedures were carried out in the dark. The gray bar indicates the levels of all-*trans*-retinyl esters in wild-type mice. Mean ± S.D. was indicated (n=3 for each point).

Figure 2. Clearance of Ret-NH_2 in the liver, blood, and eye. The 48 h dark-adapted C57BL/6 mice were gavaged with a single dose of Ret-NH_2 (1.75, 3.5, or 17.5 μmol). After gavage, the levels of Ret-NH_2 and *N*-retinylpalmitamide were measured in the liver (A, D), blood (B, E), and eye (C, F) at various time points. Retinoids were analyzed using HPLC methods as described in Materials and Methods. Mean ± S.D. was indicated (n=3 for each point).

Figure 3. Comparison of the effect of Ret-NH_2 and other inhibitors on the retinoid cycle. The 48 h dark-adapted C57BL/6 mice were gavaged with a single dose of *N*-retinylamides, Ret-NH_2, fenretinide, or 13-*cis*-retinoic acid (0.35, 1.75, or 3.5 μmol). The

Molecular Pharmacology Fast Forward. Published on July 12, 2006 as DOI: 10.1124/mol.106.026823
This article has not been copyedited and formatted. The final version may differ from this version.

mice were exposed to background light at 150 cd·m^{-2} for 20 min at 24 h after gavage. 11-*cis*-retinal in the eye and Ret-NH_2 in the liver were analyzed at 5 h (A; eye) (C; liver) and 24 h (B; eye) (D; liver) after the bleach. Retinoids were analyzed using HPLC methods as described in Materials and Methods. Mean ± S.D. was indicated (n=3 for each point).

Figure 4. Gene array analysis. The expression levels of mRNA were compared between mice treated with 13-*cis*-retinoic acid, fenretinide, and Ret-NH_2 using a 37,364 cDNA array (provided by NimbleGen System Inc.) as described in Materials and Methods. Normalized values of mRNA expression were plotted, control vs. each treated group for liver mRNA (upper panels) and for eye mRNA (lower panels) as scattered plot with Sigma Plot ver.9.0. Numbers of genes for which expression level was changed to less than 0.5 of control (dark blue points) or to more than 2 after the treatment (red points) were indicated, while the levels of expression within the experimental error is shown in light blue.

Figure 5. Deficiencies of arrestin and transducin α-subunit translocation in Ret-NH_2 treated mice. Left column indicates the mice without Ret-NH_2 administration and right column shows the mice gavaged with Ret-NH_2. A). Immunofluorescent localization of rod arrestin (red). In the dark adapted retinas, arrestin was distributed throughout the retina. Under light adapted conditions, translocation of arrestin to photoreceptor outer segments (OS) was observed in control mice (left, bottom). Only minimal translocation of arrestin to OS was observed in light adapted mice gavaged with Ret-NH_2. B). Immunofluorescent localization of transducin α-subunit (red). In the dark adapted retinas,

Molecular Pharmacology Fast Forward. Published on July 12, 2006 as DOI: 10.1124/mol.106.026823
This article has not been copyedited and formatted. The final version may differ from this version.

transducin α is localized in photoreceptor OSs. In light adapted retinas of control mice (bottom left), transducin is localized in IS, ONL, and OPL. This light-dependent translocation is mostly abolished in mice gavaged with Ret-NH_2, which shows the transducin α immunoreactivity mostly in OS and weakly in OPL. Abbreviations: OS, outer segment; IS, inner segment; ONL, outer nuclear layer; OPL, outer plexiform layer; INL, inner nuclear layer; IPL, inner plexiform layer, GCL, ganglion cell layer. Nuclei are stained with Hoechst 33342 (blue).

Figure 6. Substitution of 11-*cis*-retinal by 9-*cis*-retinal. The 48 h dark-adapted C57BL/6 mice were gavaged once with Ret-NH_2 (3.5 μmoles or 17.5 μmol), and 16 h after gavage the mice were exposed to background light at 500 $cd \cdot m^{-2}$ for 24 min. Next, mice were placed in the dark and 2 h after exposure to light gavaged with 9-*cis*-retinyl acetate (7.0 μmol) and kept in the dark prior the retinoid analysis. 9-*cis*-Retinal (A; upper panel) and 11-*cis*-retinal (A; lower panel) levels were analyzed by HPLC as described in Materials and Methods. Mean ± S.D. was indicated (n=3 for each point). Two days after 9-*cis*-retinyl acetate gavage, scotopic and photopic ERG was performed as described in Materials and Methods. Three mice from each group were examined, and representative scotopic waves were indicated (B).

Figure 7. The protective effect of Ret-NH_2 on light-induced retinal damage in a mouse model. The 48 h dark-adapted Balb/c mice were gavaged once with Ret-NH_2 (3.5 μmoles). After 16 h, mice were exposed to 5000 lux fluorescent light for 2 h to induce light damage of the retina. For the remaining time, mice were kept in the dark. A).

Molecular Pharmacology Fast Forward. Published on July 12, 2006 as DOI: 10.1124/mol.106.026823
This article has not been copyedited and formatted. The final version may differ from this version.

Morphology of the retina was examined 7 days after the light exposure. Left, the retina section from the control mouse not exposed to the intense light; middle, the retina section from mouse exposed to the intense light but treated with Ret-NH_2; right, the retina section from the control mouse exposed to the intense light treated with vehicle solution only. Similar results were obtained from 4 independent experiments. B). Retinoid content of the eyes from mice treated and exposed to light as in A. The eyes were analyzed for retinoid content two weeks after the light exposure as described in Materials and Methods. The black arrows indicate all-*trans*-retinyl ester and the open arrows indicate 11-*cis*-retinal in the chromatograms of retinoid analysis. C). Rhodopsin concentration was measured two weeks after the light exposure. D). Immunoblot of rhodopsin from the light damage induced mouse eyes with or without Ret-NH_2 treatment. Rhodopsin monomer and dimer were detected in control and Ret-NH_2 pretreated mice, whereas aggregated rhodopsin was detected in the mice treated with vehicle solution. E-H) Mice were dark-adapted for 48 h, and scotopic (E, F) and photopic (G, H) ERG was recorded 7 days after light exposure as described in Materials and Methods. Ret-NH_2 treated mice showed no significant differences compared with the control, whereas the amplitudes in mice treated with vehicle solutions were attenuated significantly compared with control and Ret-NH_2 treated mice ($P<0.0001$). Statistical analysis was performed by one-way ANOVA (n=5 in each condition).

Molecular Pharmacology Fast Forward. Published on July 12, 2006 as DOI: 10.1124/mol.106.026823
This article has not been copyedited and formatted. The final version may differ from this version.

12. Tables pages

Table 1. Retinoic acid production in the liver[a].

Gavage	all-*trans*-retinoic acid (pmol±S.D /125mg liver)							
	No treated	2 h	4 h	8 h	24 h	72 h	1 w	6 w
Ret-NH_2 (1.75 μmol)	0±0	0±0	0±0	0±0	0±0	0±0	0±0	-
Ret-NH_2 (3.5 μmol)	0±0	0±0	0±0	0±0	0±0	0±0	0±0	0±0
Ret-NH_2 (17.5 μmol)	0±0	2.8±0.9	4.2±1.2	3.4±1.6	0±0	0±0	0±0	-
Fenretinide (17.5 μmol)	0±0	6.8±0.8	12.9±0.67	4.6±0.5	0±0	0±0	-	-
all-*trans*-ROL (17.5 μmol)	0±0	449.6±37.9	1,567.6±565.4	54.9±41.8	1.3±2.2	0±0	0±0	-

[a]Retinoids were analyzed as described in Materials and Methods.

Molecular Pharmacology Fast Forward. Published on July 12, 2006 as DOI: 10.1124/mol.106.026823
This article has not been copyedited and formatted. The final version may differ from this version.

Table 2. Rhodopsin amounts of LD (light damaged) mice[a].

	no light	LD induced	
		with Ret-NH_2	without Ret-NH_2
rhodopsin (pmol/eye)	476 ± 32	417 ± 55	82 ± 24***

[a]Rhodopsin was analyzed as described in Materials and Methods.

***, P<0.0001

Figure 1

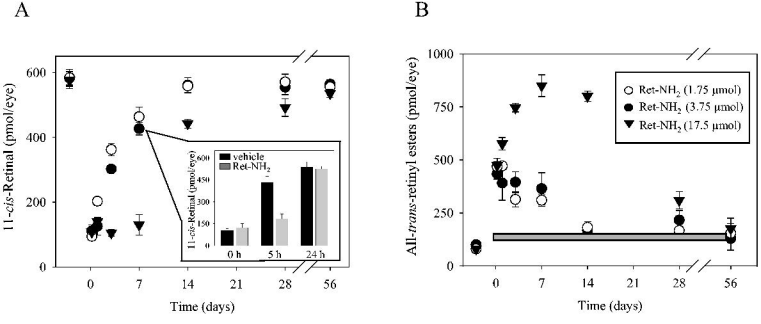
A
11-cis-Retinal (pmol/eye)
600
400
200
0
0
7
14
21
28
56
Time (days)
vehicle
Ret-NH2
11-cis-Retinal (pmol/eye)
600
450
300
150
0
0 h
5 h
24 h
B
All-trans-retinyl esters (pmol/eye)
1000
750
500
250
0
Ret-NH2 (1.75 μmol)
Ret-NH2 (3.75 μmol)
Ret-NH2 (17.5 μmol)
0
7
14
21
28
56
Time (days)

Figure 2

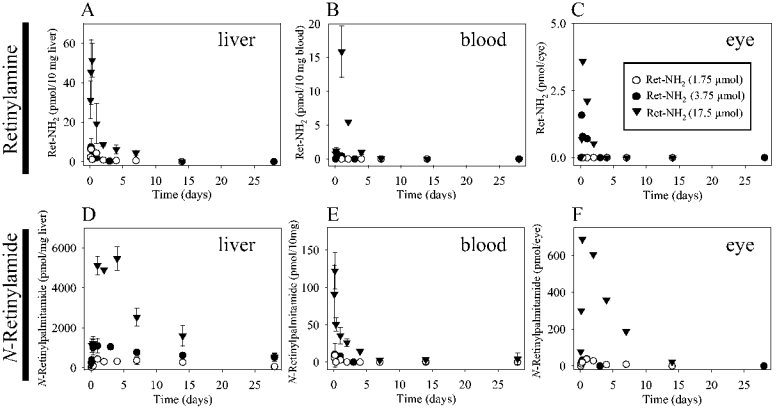
Retinylamine
N-Retinylamide
A
liver
Ret-NH2 (pmol/10 mg liver)
Time (days)
B
blood
Ret-NH2 (pmol/10 mg blood)
Time (days)
C
eye
Ret-NH2 (pmol/eye)
Ret-NH2 (1.75 µmol)
Ret-NH2 (3.75 µmol)
Ret-NH2 (17.5 µmol)
Time (days)
D
liver
N-Retinylpalmitamide (pmol/mg liver)
Time (days)
E
blood
N-Retinylpalmitamide (pmol/10mg)
Time (days)
F
eye
N-Retinylpalmitamide (pmol/eye)
Time (days)

Figure 3

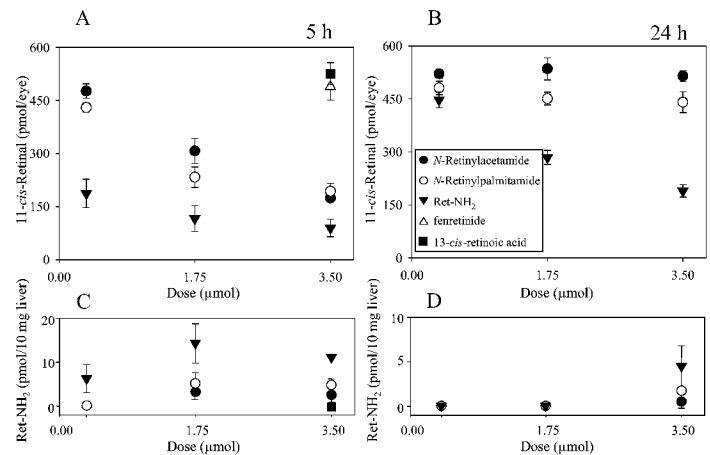
A
5 h
B
24 h
11-cis-Retinal (pmol/eye)
600
450
300
150
0
0.00
1.75
3.50
Dose (μmol)
N-Retinylacetamide
N-Retinylpalmitamide
Ret-NH2
fenretinide
13-cis-retinoic acid
C
D
Ret-NH2 (pmol/10 mg liver)
20
10
5

Figure 4

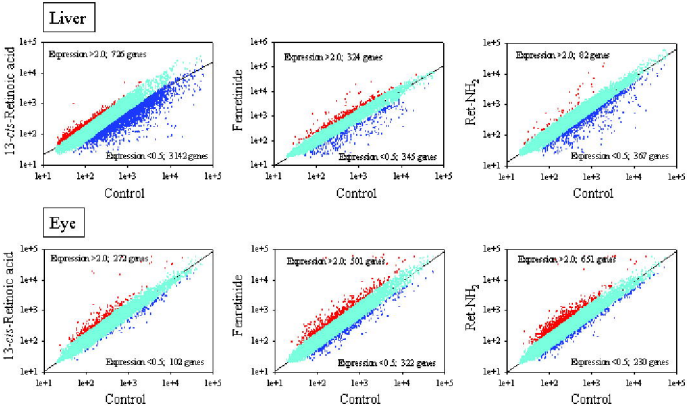
Liver
13-cis-Retinoic acid
Expression >2.0; 926 genes
Expression <0.5; 3142 genes
Control
Fenretinide
Expression >2.0; 324 genes
Expression <0.5; 345 genes
Control
Ret-NH2
Expression >2.0; 62 genes
Expression <0.5; 367 genes
Control
Eye
13-cis-Retinoic acid
Expression >2.0; 272 genes
Expression <0.5; 102 genes
Control
Fenretinide
Expression >2.0; 301 genes
Expression <0.5; 322 genes
Control
Ret-NH2
Expression >2.0; 651 genes
Expression <0.5; 230 genes
Control

Figure 5

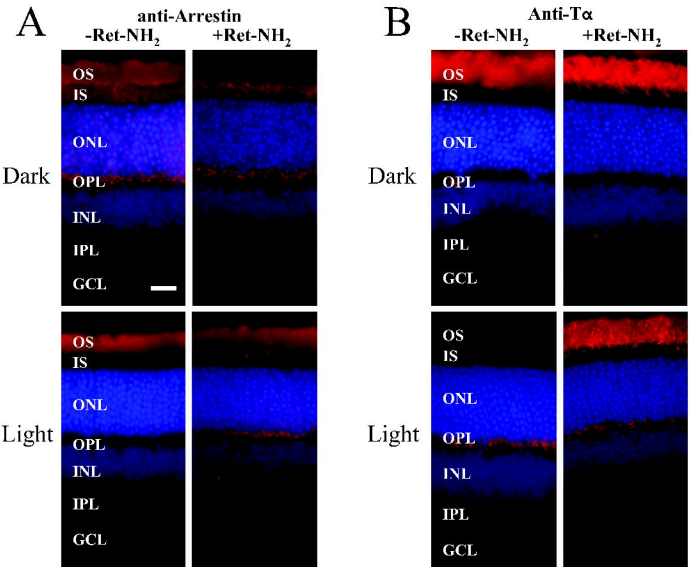
A
anti-Arrestin
-Ret-NH2
+Ret-NH2
Dark
Light
OS
IS
ONL
OPL
INL
IPL
GCL
B
Anti-Tα
-Ret-NH2
+Ret-NH2
Dark
Light
OS
IS
ONL
OPL
INL
IPL
GCL

Figure 6

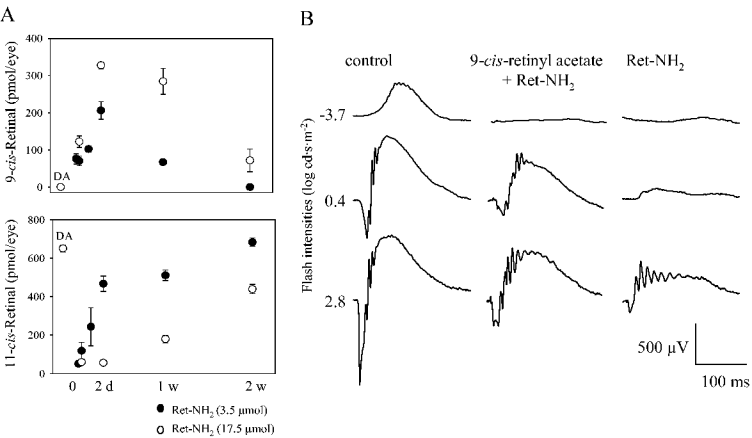
A
400
300
200
100
0
9-cis-Retinal (pmol/eye)
DA
800
600
400
200
0
11-cis-Retinal (pmol/eye)
DA
0
2 d
1 w
2 w
Ret-NH2 (3.5 μmol)
Ret-NH2 (17.5 μmol)
B
control
9-cis-retinyl acetate
+ Ret-NH2
Ret-NH2
-3.7
0.4
2.8
Flash intensities (log cd·s·m-2)
500 μV
100 ms

Figure 7

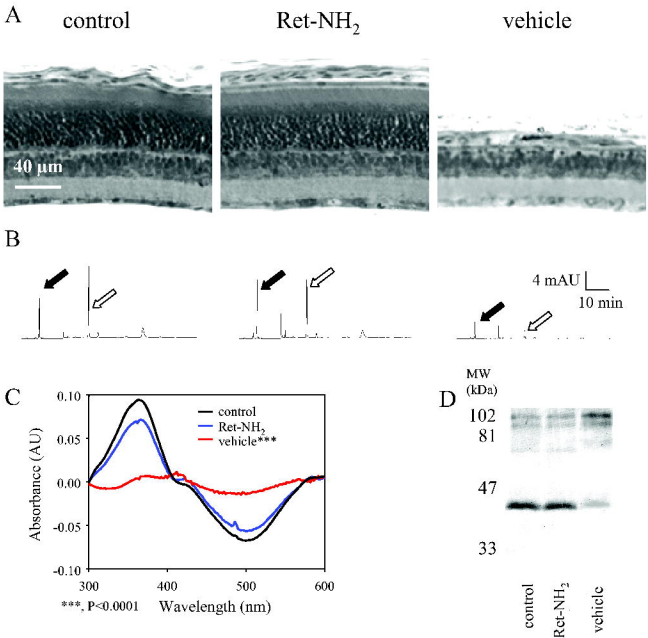
A
control
Ret-NH2
vehicle
40 µm
B
4 mAU
10 min
C
0.10
0.05
0.00
-0.05
-0.10
Absorbance (AU)
control
Ret-NH2
vehicle***
300
400
500
600
***, P<0.0001
Wavelength (nm)
D
MW
(kDa)
102
81
47
33
control
Ret-NH2
vehicle

Figure 7

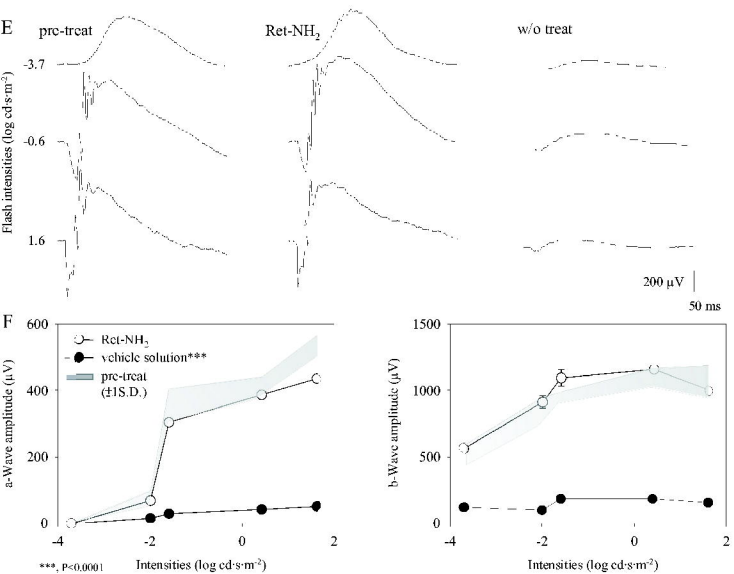
E
pre-treat
Ret-NH2
w/o treat
-3.7
-0.6
1.6
Flash intensities (log cd·s·m-2)
200 μV
50 ms
F
Ret-NH2
vehicle solution***
pre-treat
(±1S.D.)
a-Wave amplitude (μV)
b-Wave amplitude (μV)
***, P<0.0001
Intensities (log cd·s·m-2)
Intensities (log cd·s·m-2)

Figure 7

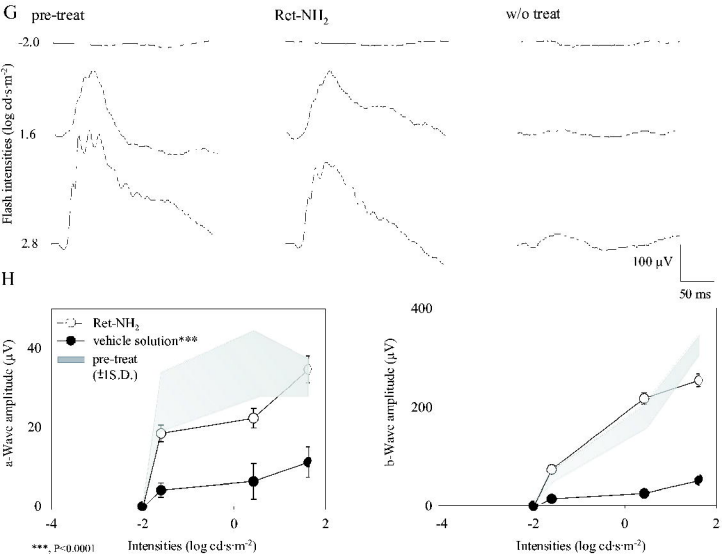
G
pre-treat
Ret-NH2
w/o treat
-2.0
1.6
2.8
Flash intensities (log cd·s·m-2)
100 μV
50 ms
H
Ret-NH2
vehicle solution***
pre-treat
(±1S.D.)
a-Wave amplitude (μV)
40
20
0
-4
-2
0
2
***, P<0.0001
Intensities (log cd·s·m-2)
400
200
0
b-Wave amplitude (μV)
-4
-2
0
2
Intensities (log cd·s·m-2)

SUPPLEMENT

Figure S1. Time-dependent efficacy of Ret-acetamide in inhibition of the chromophore production. The 48 h dark-adapted C57BL/6 mice were gavaged once with Ret-acetamide (0.35 μmol) and then exposed to intense light for 3 min at 500 $cd \cdot m^{-2}$ (bleaching of ~50% of rhodopsin) at various times after gavage. 11-*cis*-Retinal level was analyzed after 60 min of dark adaptation using HPLC methods as described in Materials and Methods. Mean ± S.D. was indicated (n=3 in each condition).

Figure S2. Efficacy at peak blood concentration of Ret-acetamide treatment. The 48 h dark-adapted C57BL/6 mice were gavaged once with Ret-acetamide (amounts as indicated) and then exposed to intense light for 24 min at 500 $cd \cdot m^{-2}$ (bleaching of ~80% of rhodopsin) at 7.5 h after gavage. Mice were dark-adapted for 48 h and gavaged with various doses of Ret-acetamide, and then exposed to intense light for 12 min at 500 $d \cdot m^{-2}$. 11-*cis*-retinal level was analyzed after 60 min of dark adaptation using HPLC methods as described in Materials and Methods. Mean ± S.D. was indicated (n=3 in each condition).

Figure S3. The effect of multiple gavages of Ret-NH_2 on retinoid levels in the eye, body weight, and visual responses. The 48 h dark-adapted C57BL/6 mice were gavaged four times at 7 day-intervals with Ret-NH_2 (3.5 μmoles). Mice were kept in a 12 h light/12 h dark cycle, and retinoid analysis was performed after mice were 24 h dark adapted before analysis. A). All-*trans*-retinyl esters and 11-*cis*-retinal levels in the eye. The retinoid analysis was performed 7 days, one month, and two months after the final gavage. B). ERG analysis. Mice were dark-adapted for 24 h, and scotopic and photopic ERG was recorded 7 days and two months after the final gavage as described in Materials and Methods. A-wave (a and c) and b-wave (b and f) are shown 7 days after gavage in scotopic conditions and in photopic conditions, respectively. A-wave (a and c) and b-wave (b and f) are shown 1 week post-gavage in scotopic conditions and in photopic conditions, respectively. A-wave (e and g) and b-wave (f and h) are shown 2 months post-gavage in scotopic conditions and in photopic conditions, respectively (n = 5 for each conditions). The responses from Ret-NH_2 treated mice were attenuated slightly in scotopic conditions and significantly in photopic conditions at high intensitiy stimulations

(c and d, $P<0.01$) 1 week after gavage. Those responses recovered to compatible levels with control mice at 2 months post treatment. Statistical analysis was performed by one-way ANOVA. Error bar was indicated. C). Body weight of treated mice as a function of time. Mean±S.D. was indicated.

Figure S4. A long-term suppression of 11-*cis*-retinal production by Ret-NH_2. The 48 h dark-adapted C57BL/6 mice were gavaged with a single dose of Ret-NH_2 (1, 75 or 3.5 μmol). Mice were kept in the dark for 16 h, and exposed to background illumination that bleached 80% of rhodopsin (reduction in 11-*cis*-retinal) and transferred to dark for the remaining time of the experiment. The first retinoid analysis was done 5 h after the exposure to light. Additional gavages were performed on the days 1, 3, and 5 after the mice were exposed to light and the retinoid analysis was performed on days 1, 3, 5, and 7. Three mice were examined at each time point. Mean ± S.D. was indicated (n = 5 for each conditions).

Figure S5. Analysis of protein levels by immunoblotting. Mice were dark adapted for 48 h and gavaged with 2 μmol of 13-*cis*-retinoic acid, fenretinide, or Ret-NH_2. The mice were kept in the dark for 16 h after the gavage and retinas were collected under dim light. The retinas were homogenized in 500 μl of 100 mM sodium phosphate, pH 7.0, containing 1 mM *n*-dodecyl-β-maltoside. The homogenates (10 μg total proteins) were loaded onto the SDS gel and immunoblotting was carried out as described in the Materials and Methods.

Table 1, supplement. The largest changes in gene expression after retinoid treatment in the liver. [a]

Inhibitor	Fold of induction (mean±SD)	Unigene	GenBank Description
Ret-NH_2			
	Increased		
	4.28±0.11	Mm.1262	Cytochrome P450, family 17, subfamily a, polypeptide 1 (Cyp17a1) , mRNA
	7.89±0.11	Mm.14413	Cytochrome P450, family 2, subfamily b, polypeptide 9 (Cyp2b9)
	4.4±0.083	Mm.10742	Cytochrome P450, family 4, subfamily a, polypeptide 10, mRNA (cDNA clone MGC:18335 IMAGE:4242518)
	6.23±0.46	Mm.250901	Cytochrome P450, family 4, subfamily a, polypeptide 14 (Cyp4a14), mRNA
	4.28±0.11	Mm.2900	Flavin containing monooxygenase 3 (Fmo3), mRNA
	10.53±1.19	Mm.370234	Hepcidin antimicrobial peptide 2, mRNA (cDNA clone MGC:107568 IMAGE:6765293)
	4.67±0.72	Mm.9537	Lipocalin 2 (Lcn2), mRNA
	12.18±3.31	Mm.192991	Metallothionein 1, mRNA (cDNA clone MGC:47147 IMAGE:4990006)
	6.26±0.11	Mm.147226	Metallothionein 2, mRNA (cDNA clone MGC:19383 IMAGE:2651471)
	6.08±0.81	Mm.260026	Sulfotransferase family 2A, dehydroepiandrosterone (DHEA)-preferring, member 2 (Sult2a2), mRNA
	Decreased		
	0.16±0.047	Mm.333096	Breast cancer resistance protein 1 (Bcrp1)
	0.18±0.036	Mm.20247	Complement component 6, mRNA (cDNA clone MGC:18813 IMAGE:4196330)
	0.13±0.085	Mm.378904	Cytochrome P450, family 2, subfamily d, polypeptide 9, mRNA (cDNA clone MGC:11540 IMAGE:3964178)
	0.13±0.055	Mm.215544	Cytochrome P450, family 4, subfamily x, polypeptide 1 (Cyp4x1), mRNA
	0.071±0.0074	Mm.316000	Cytochrome P450, family 7, subfamily b, polypeptide 1, mRNA (cDNA clone MGC:46910 IMAGE:5098739)
	0.097±0.0034	Mm.21806	Elongation of very long chain fatty acids (FEN1/Elo2, SUR4/Elo3, yeast)-like 3, mRNA (cDNA clone MGC:18360 IMAGE:4196583)
	0.085±0.0074	Mm.242728	Germ cell nuclear factor protein (Nr6a1)
	0.17±0.0098	Mm.378930	Glutathione S-transferase, pi 1, mRNA (cDNA clone MGC:6054 IMAGE:3593257)
	0.19±0.011	Mm.281298	Growth arrest and DNA-damage-inducible 45 gamma, mRNA (cDNA clone MGC:5695 IMAGE:3493618)
	0.09±0.0085	Mm.17910	Hydroxysteroid dehydrogenase-5, delta<5>-3-beta, mRNA (cDNA clone MGC:14041 IMAGE:4193717)

	0.06±0.0067	Mm.237772	Major urinary protein 1, mRNA (cDNA clone MGC:46757 IMAGE:4161709)
	0.15±0.0078	Mm.366415	Major urinary protein 2, mRNA (cDNA clone MGC:18535 IMAGE:4196403)
	0.13±0.013	Mm.250267	Major urinary protein 3, mRNA (cDNA clone MGC:28540 IMAGE:4194688)
	0.12±0.0096	Mm.34335	Major urinary protein 4, mRNA (cDNA clone MGC:18534 IMAGE:4190774)
	0.13±0.014	Mm.386768	Major urinary protein 5 (Mup5), mRNA
	0.16±0.045	Mm.103665	Organic anion transporting polypeptide 1
	0.19±0.024	Mm.358950	Reverse transcriptase (LOC277923), mRNA
	0.15±0.0067	Mm.36758	RIKEN cDNA 1110028A07 gene, mRNA (cDNA clone IMAGE:3663008)
	0.18±0.0098	Mm.276106	Similar to cytochrome P450, 4a10, mRNA (cDNA clone MGC:37891 IMAGE:5101821)
	0.15±0.013	Mm.11223	Similar to hypothetical protein MGC37588, mRNA (cDNA clone MGC:28125 IMAGE:3980327)
	0.078±0.0087	Mm.291725	Similar to spermiogenesis specific transcript on the Y 2 (LOC435023), mRNA
	0.068±0.0063	Mm.358638	Simple repeat sequence-containing transcript (Srst), mRNA
	0.082±0.0078	Mm.26741	UDP glucuronosyltransferase 2 family, polypeptide B1 (Ugt2b1), mRNA
fenretinide			
	Increased		
	5.01±0.16	Mm.295456	ATP-binding cassette, sub-family D (ALD), member 2, mRNA (cDNA clone MGC:29110 IMAGE:5027149)
	7.12±2.43	Mm.19131	Complement component 3 (C3), mRNA
	5.36±1.08	Mm.133179	Cytochrome P450, CYP3A
	6.17±0.88	Mm.218749	Cytochrome P450, family 2, subfamily b, polypeptide 10 (Cyp2b10), transcript variant 1, mRNA
	12.73±0.18	Mm.14413	Cytochrome P450, family 2, subfamily b, polypeptide 9 (Cyp2b9), mRNA
	8.01±0.69	Mm.10742	Cytochrome P450, family 4, subfamily a, polypeptide 10, mRNA (cDNA clone MGC:18335 IMAGE:4242518)
	10.11±0.74	Mm.250901	Cytochrome P450, family 4, subfamily a, polypeptide 14 (Cyp4a14), mRNA
	8.24±0.21	Mm.2900	Flavin containing monooxygenase 3 (Fmo3), mRNA
	12.59±2.28	Mm.370234	Hepcidin antimicrobial peptide 2, mRNA (cDNA clone MGC:107568 IMAGE:6765293)
	7.01±0.57	Mm.347700	Histone 1, H2ae, mRNA (cDNA clone MGC:90847 IMAGE:5713252)
	22.71±6.16	Mm.192991	Metallothionein 1, mRNA (cDNA clone MGC:47147 IMAGE:4990006)
	8.05±0.16	Mm.147226	Metallothionein 2, mRNA (cDNA clone MGC:19383

			IMAGE:2651471)
	14.14±1.89	Mm.260026	Sulfotransferase family 2A, dehydroepiandrosterone (DHEA)-preferring, member 2 (Sult2a2), mRNA
	4.35±0.2	Mm.6590	Sulfotransferase family 3A, member 1 (Sult3a1), mRNA
	Decreased		
	0.12±0.034	Mm.254873	C-type lectin domain family 2, member g (Clec2g), mRNA
	0.19±0.044	Mm.378904	Cytochrome P450, family 2, subfamily d, polypeptide 9, mRNA (cDNA clone MGC:11540 IMAGE:3964178)
	0.094±0.013	Mm.215544	Cytochrome P450, family 4, subfamily x, polypeptide 1 (Cyp4x1), mRNA
	0.079±0.045	Mm.316000	Cytochrome P450, family 7, subfamily b, polypeptide 1, mRNA (cDNA clone MGC:46910 IMAGE:5098739)
	0.096±0.0087	Mm.21806	Elongation of very long chain fatty acids (FEN1/Elo2, SUR4/Elo3, yeast)-like 3, mRNA (cDNA clone MGC:18360 IMAGE:4196583)
	0.19±0.011	Mm.250909	Eukaryotic translation initiation factor 2, subunit 3, structural gene Y-linked (Eif2s3y), mRNA
	0.079±0.0099	Mm.242728	Germ cell nuclear factor protein (Nr6a1)
	0.19±0.041	Mm.281298	Growth arrest and DNA-damage-inducible 45 gamma, mRNA (cDNA clone MGC:5695 IMAGE:3493618)
	0.099±0.024	Mm.17910	Hydroxysteroid dehydrogenase-5, delta<5>-3-beta, mRNA (cDNA clone MGC:14041 IMAGE:4193717)
	0.034±0.0031	Mm.237772	Major urinary protein 1, mRNA (cDNA clone MGC:46757 IMAGE:4161709)
	0.19±0.041	Mm.386768	Major urinary protein 5 (Mup5), mRNA
	0.16±0.0074	Mm.31748	NADPH oxidase 4, mRNA (cDNA clone MGC:29375 IMAGE:5044835)
	0.12±0.0066	Mm.377112	Per-hexamer repeat gene 5 (Phxr5), mRNA
	0.13±0.041	Mm.358950	Reverse transcriptase (LOC277923), mRNA
	0.11±0.067	Mm.362038	RIKEN cDNA 2310043N13 gene, mRNA (cDNA clone MGC:107477 IMAGE:30089818)
	0.19±0.031	Mm.104955	Serine protease inhibitor, Kunitz type 1, mRNA (cDNA clone MGC:6844 IMAGE:2650110)
	0.072±0.0088	Mm.276106	Similar to cytochrome P450, 4a10, mRNA (cDNA clone MGC:37891 IMAGE:5101821)
	0.058±0.0096	Mm.11223	Similar to hypothetical protein MGC37588, mRNA (cDNA clone MGC:28125 IMAGE:3980327)
	0.029±0.01	Mm.291725	Similar to spermiogenesis specific transcript on the Y 2 (LOC435023), mRNA
	0.027±0.0074	Mm.358638	Simple repeat sequence-containing transcript (Srst), mRNA
	0.093±0.0037	Mm.347498	Spermiogenesis specific transcript on the Y 1 (Ssty1), mRNA
	0.17±0.034	Mm.220165	Zinc finger protein 353 (Zfp353), mRNA
13-*cis*-retinoic			

acid			
	Increased		
	5.48±1.49	Mm.192991	Metallothionein 1
	4.3±1.28	Mm.375125	Non-allelic mRNA for pancreatic alpha-amylase isozyme 3' end
	4.32±1.12	Mm.141312	Procollagen, type IX, alpha 3
	4.71±1.23	Mm.304354	Sycp3 like Y-linked (Sly), mRNA
	Decreased		
	0.059±0.0059	Mm.378885	ATP synthase, H+ transporting, mitochondrial F0 complex, subunit b, isoform 1, mRNA (cDNA clone MGC:107569 IMAGE:6756180)
	0.097±0.0031	Mm.250866	Ahd-2=acetaldehyde dehydrogenase [mice, BALB/c, livers, mRNA Partial, 1632 nt]
	0.056±0.00056	Mm.378904	Cytochrome P450, family 2, subfamily d, polypeptide 9, mRNA (cDNA clone MGC:11540 IMAGE:3964178)
	0.094±0.0046	Mm.215544	Cytochrome P450, family 4, subfamily x, polypeptide 1 (Cyp4x1), mRNA
	0.071±0.0068	Mm.316000	Cytochrome P450, family 7, subfamily b, polypeptide 1, mRNA (cDNA clone MGC:46910 IMAGE:5098739)
	0.098±0.0026	Mm.273403	Cytochrome c oxidase, subunit Va, mRNA (cDNA clone MGC:36114 IMAGE:5372849)
	0.091±0.0088	Mm.28191	Carboxylesterase 2 (Ces2), mRNA
	0.098±0.0027	Mm.379940	Complement component factor h, mRNA (cDNA clone IMAGE:5132971)
	0.094±0.0094	Mm.29046	CDNA sequence BC027342 (BC027342), mRNA
	0.057±0.01	Mm.88078	Esterase 1, mRNA (cDNA clone MGC:18575 IMAGE:4196339)
	0.091±0.0075	Mm.295534	Esterase 31, mRNA (cDNA clone MGC:74105 IMAGE:30315941)
	0.071±0.0057	Mm.22126	Fatty acid binding protein 1, liver, mRNA (cDNA clone MGC:13855 IMAGE:4159971)
	0.043±0.0047	Mm.242728	Germ cell nuclear factor protein (Nr6a1)
	0.099±0.0063	Mm.378930	Glutathione S-transferase, pi 1, mRNA (cDNA clone MGC:6054 IMAGE:3593257)
	0.078±0.0034	Mm.17910	Hydroxysteroid dehydrogenase-5, delta<5>-3-beta, mRNA (cDNA clone MGC:14041 IMAGE:4193717)
	0.082±0.0034	Mm.261676	Histone 1, H2bc, mRNA (cDNA clone MGC:30336 IMAGE:3993954)
	0.0046±0.024	Mm.237772	Major urinary protein 1, mRNA (cDNA clone MGC:46757 IMAGE:4161709)
	0.042±0.0079	Mm.250267	Major urinary protein 3, mRNA (cDNA clone MGC:28540 IMAGE:4194688)
	0.082±0.0034	Mm.386768	Major urinary protein 5 (Mup5), mRNA
	0.03±0.0021	Mm.366415	Major urinary protein 2, mRNA (cDNA clone MGC:18535 IMAGE:4196403)
	0.082±0.0085	Mm.34869	NADH dehydrogenase (ubiquinone) 1 alpha subcomplex, 1, mRNA

			(cDNA clone MGC:35935 IMAGE:5031206)
	0.095±0.0087	Mm.42805	NADH dehydrogenase (ubiquinone) Fe-S protein 5, mRNA (cDNA clone MGC:7315 IMAGE:3485964)
	0.085±0.0037	Mm.27889	Nudix (nucleoside diphosphate linked moiety X)-type motif 7 (Nudt7), transcript variant 2, mRNA
	0.031±0.0045	Mm.121265	Proteasome (prosome, macropain) subunit, alpha type 1, mRNA (cDNA clone MGC:6546 IMAGE:2655483)
	0.089±0.0066	Mm.27066	Phytanoyl-CoA hydroxylase, mRNA (cDNA clone MGC:5835 IMAGE:3489939)
	0.097±0.0078	Mm.379127	Proteasome (prosome, macropain) 26S subunit, ATPase, 6, mRNA (cDNA clone IMAGE:2812662)
	0.09±0.0065	Mm.279782	Peroxiredoxin 5, mRNA (cDNA clone IMAGE:3585739)
	0.063±0.0087	Mm.358667	Receptor (calcitonin) activity modifying protein 2 (Ramp2), mRNA
	0.084±0.0086	Mm.45980	Ring finger protein 125, mRNA (cDNA clone IMAGE:5317267)
	0.097±0.0073	Mm.358950	Reverse transcriptase (LOC277923), mRNA
	0.064±0.0033	Mm.358638	Simple repeat sequence-containing transcript (Srst), mRNA
	0.038±0.0083	Mm.291725	Similar to spermiogenesis specific transcript on the Y 2 (LOC435023), mRNA
	0.047±0.0086	Mm.250980	Solute carrier family 38, member 4, mRNA (cDNA clone MGC:37778 IMAGE:5097293)
	0.048±0.0069	Mm.11223	Similar to hypothetical protein MGC37588, mRNA (cDNA clone MGC:28125 IMAGE:3980327)
	0.058±0.0064	Mm.276106	Similar to cytochrome P450, 4a10, mRNA (cDNA clone MGC:37891 IMAGE:5101821)
	0.091±0.0098	Mm.104955	Serine protease inhibitor, Kunitz type 1, mRNA (cDNA clone MGC:6844 IMAGE:2650110)
	0.095±0.0061	Mm.272223	Solute carrier organic anion transporter family, member 1b2 (Slco1b2), transcript variant 1, mRNA
	0.096±0.006	Mm.347498	Spermiogenesis specific transcript on the Y 1 (Ssty1), mRNA
	0.098±0.0085	Mm.218639	Sulfiredoxin 1 homolog (S. cerevisiae) (Srxn1), mRNA
	0.037±0.0091	Mm.246377	Tubulin, beta 2, mRNA (cDNA clone IMAGE:2650284)
	0.08±0.0065	Mm.258622	Tryptophan 2,3-dioxygenase, mRNA (cDNA clone MGC:25811 IMAGE:4159877)
	0.086±0.011	Mm.379065	Tocopherol (alpha) transfer protein, mRNA (cDNA clone IMAGE:3990597)
	0.037±0.0012	Mm.26741	UDP glucuronosyltransferase 2 family, polypeptide B1 (Ugt2b1), mRNA

[a]-the analysis was carried out as described in the Material and Methods.

Table 2, supplement. The largest changes in gene expression after retinoid treatment in the eye. [a]

Inhibitor	Fold of induction (mean±SD)	Unigene	GenBank Description
Ret-NH_2			
	Increased		
	274.63±43.55	Mm.258170	Crystallin, gamma E (Cryge), mRNA
	79.65±11.35	Mm.275362	Crystallin, gamma F (Crygf), mRNA
	55.59±7.78	Mm.26904	Crystallin, gamma A, mRNA (cDNA clone MGC:66631 IMAGE:6824353)
	24.92±4.91	Mm.378900	Crystallin, gamma D (Crygd), mRNA
	16.64±2.22	Mm.298885	Crystallin, gamma C (Crygc), mRNA
	7.63±1.41	Mm.340132	Myosin heavy chain IIX (MYHC-IIX gene)
	7.01±1.33	Mm.358667	Receptor (calcitonin) activity modifying protein 2 (Ramp2), mRNA
	6.05±0.97	Mm.178246	Chromodomain helicase DNA binding protein 3, mRNA (cDNA clone MGC:40857 IMAGE:5369285)
	5.77±0.95	Mm.247113	Ribosomal protein L30, mRNA (cDNA clone MGC:6114 IMAGE:3489311)
	5.24±0.37	Mm.741	Fatty acid binding protein 5, epidermal, mRNA (cDNA clone MGC:5786 IMAGE:3490535)
	5.06±0.67	Mm.358643	Troponin T1, skeletal, slow (Tnnt1), mRNA
	5.03±0.78	Mm.378899	Crystallin, beta B3, mRNA (cDNA clone MGC:25487 IMAGE:4501690)
	4.48±0.31	Mm.12848	Signal recognition particle 54, mRNA (cDNA clone MGC:30254 IMAGE:3708250)
	4.74±0.77	Mm.3110	Kinectin 1 (Ktn1), mRNA
	4.67±0.63	Mm.205190	Myeloid/lymphoid or mixed-lineage leukemia 5, mRNA (cDNA clone IMAGE:30605195)
	4.61±0.74	Mm.29586	Brain abundant, membrane attached signal protein 1 (Basp1), mRNA
	4.54±0.66	Mm.220038	DEAD (Asp-Glu-Ala-Asp) box polypeptide 5, mRNA (cDNA clone IMAGE:3598655)
	4.53±0.85	Mm.83949	Elongation of very long chain fatty acids (FEN1/Elo2, SUR4/Elo3, yeast)-like 4, mRNA (cDNA clone MGC:47132 IMAGE:4503493)
	4.43±0.32	Mm.223744	Kinesin family member 5B (Kif5b), mRNA
	4.36±0.41	Mm.29742	CD24a antigen (Cd24a), mRNA
	4.19±0.32	Mm.209385	Mortality factor 4 like 1, mRNA (cDNA clone MGC:27701 IMAGE:4923923)
	4.19±0.21	Mm.233117	Aldehyde dehydrogenase 18 family, member A1 (Aldh18a1), transcript variant 2, mRNA

	4.08±0.65	Mm.259884	Methylmalonyl-Coenzyme A mutase, mRNA (cDNA clone MGC:29139 IMAGE:5007694)
	4.05±0.34	Mm.277354	Erbb2 interacting protein, mRNA (cDNA clone IMAGE:4988135)
	Decreased		
	0.37±0.0031	Mm.12825	Retinol binding protein 2, cellular (Rbp2), mRNA
	0.4±0.0019	Mm.175661	Interferon induced transmembrane protein 1 (Ifitm1), mRNA
	0.39±0.0022	Mm.187847	Stefin A2 like 1 (Stfa2l1), mRNA
	0.31±0.0022	Mm.21855	Peptidoglycan recognition protein 1, mRNA (cDNA clone MGC:11430 IMAGE:3969014)
	0.3±0.0034	Mm.22742	FXYD domain-containing ion transport regulator 2, mRNA (cDNA clone MGC:25914 IMAGE:4222609)
	0.35±0.0063	Mm.237772	Major urinary protein 1, mRNA (cDNA clone MGC:46757 IMAGE:4161709)
	0.37±0.0014	Mm.262135	Protein kinase inhibitor beta, cAMP dependent, testis specific (Pkib), mRNA
	0.17±0.0018	Mm.270157	Melanoma antigen (Mela), mRNA
	0.35±0.0024	Mm.271275	Interferon stimulated gene 12 (Isg12)
	0.34±0.003	Mm.273277	Tripartite motif protein 29, mRNA (cDNA clone MGC:28195 IMAGE:3988926)
	0.34±0.0037	Mm.280038	S100 calcium binding protein A11 (calizzarin) (S100a11), mRNA
	0.32±0.0024	Mm.288567	Hemoglobin, beta adult major chain, mRNA (cDNA clone MGC:40691 IMAGE:3988455)
	0.39±0.0029	Mm.30181	PDZK1 interacting protein 1, mRNA (cDNA clone MGC:19227 IMAGE:4241868)
	0.41±0.0029	Mm.331185	S100 calcium binding protein A16 (S100a16), mRNA
	0.37±0.0027	Mm.347539	Placental lactogen-I beta (Plib), mRNA
	0.4±0.0022	Mm.347593	Paired immunoglobin-like type 2 receptor beta (Pilrb), mRNA
	0.36±0.0036	Mm.350930	Similar to spermiogenesis specific transcript on the Y 2, mRNA (cDNA clone MGC:118215 IMAGE:30920635)
	0.39±0.0066	Mm.354963	Proline rich protein 2 (Prp2), mRNA
	0.34±0.0041	Mm.358887	Androgen binding protein beta, mRNA (cDNA clone MGC:19070 IMAGE:4193111)
	0.33±0.0044	Mm.378975	Nerve growth factor, gamma (Ngfg), mRNA
	0.41±0.0032	Mm.380329	Immunoglobulin heavy chain (J558 family), mRNA (cDNA clone MGC:30284 IMAGE:4205959)
	0.31±0.0011	Mm.3815	Syndecan 4, mRNA (cDNA clone MGC:11456 IMAGE:3154160)
	0.16±0.001	Mm.45436	Lysozyme, mRNA (cDNA clone IMAGE:2655292)
	0.4±0.0037	Mm.6559	Asialoglycoprotein receptor 1, mRNA (cDNA clone MGC:36097 IMAGE:5102469)
fenretinide			

	Increased		
	282.67±31.64	Mm.258170	Crystallin, gamma E (Cryge), mRNA
	81.33±9.32	Mm.275362	Crystallin, gamma F (Crygf), mRNA
	51.56±4.97	Mm.26904	Crystallin, gamma A, mRNA (cDNA clone MGC:66631 IMAGE:6824353)
	26.69±3.41	Mm.378900	Crystallin, gamma D (Crygd), mRNA
	16.52±2.41	Mm.298885	Crystallin, gamma C (Crygc), mRNA
	7.72±1.42	Mm.377880	Histone 1, H2bl (Hist1h2bl), mRNA
	6.71±1.74	Mm.358955	Histone 1, H2bk (Hist1h2bk), mRNA
	6.06±1.35	Mm.378899	Crystallin, beta B3, mRNA (cDNA clone MGC:25487 IMAGE:4501690)
	5.79±1.01	Mm.358643	Troponin T1, skeletal, slow (Tnnt1), mRNA
	5.75±1.74	Mm.220038	DEAD (Asp-Glu-Ala-Asp) box polypeptide 5, mRNA (cDNA clone IMAGE:3598655)
	5.33±0.65	Mm.160040	PREDICTED: galectin-related inter-fiber protein [Mus musculus], mRNA sequence
	5.31±0.47	Mm.261670	Histone 2, H2aa1 (Hist2h2aa1), mRNA
	5.04±0.73	Mm.12848	Signal recognition particle 54, mRNA (cDNA clone MGC:30254 IMAGE:3708250)
	5.01±0.69	Mm.63484	Crystallin, gamma N (Crygn), mRNA
	4.89±0.31	Mm.358954	Histone 2, H2ab (Hist2h2ab), mRNA
	4.47±0.33	Mm.122366	Heterogeneous nuclear ribonucleoprotein F, mRNA (cDNA clone MGC:36543 IMAGE:4950131)
	4.47±0.64	Mm.21740	Heterogeneous nuclear ribonucleoprotein H1 (Hnrph1), mRNA
	4.18±0.47	Mm.3110	Kinectin 1 (Ktn1), mRNA
	Decreased		
	0.14±0.0011	Mm.44101	ATPase, Na+/K+ transporting, alpha 3 polypeptide, mRNA (cDNA clone MGC:38914 IMAGE:5362423)
	0.15±0.0017	Mm.270157	Melanoma antigen (Mela), mRNA
	0.16±0.0031	Mm.288567	Hemoglobin, beta adult major chain, mRNA (cDNA clone MGC:40691 IMAGE:3988455)
	0.21±0.0015	Mm.45436	Lysozyme, mRNA (cDNA clone IMAGE:2655292)
	0.23±0.001	Mm.297	Actin, beta, cytoplasmic (Actb), mRNA
	0.24±0.0033	Mm.233475	PREDICTED: hypothetical protein LOC75509 [Mus musculus], mRNA sequence
	0.25±0.0014	Mm.12825	Retinol binding protein 2, cellular (Rbp2), mRNA
	0.25±0.0011	Mm.262135	Protein kinase inhibitor beta, cAMP dependent, testis specific (Pkib), mRNA
	0.27±0.0016	Mm.141312	Procollagen, type IX, alpha 3, mRNA (cDNA clone MGC:32160

			IMAGE:5003028)
	0.27±0.001	Mm.299774	Junction plakoglobin, mRNA (cDNA clone MGC:103220 IMAGE:4459882)
	0.28±0.0024	Mm.358887	Androgen binding protein beta, mRNA (cDNA clone MGC:19070 IMAGE:4193111)
	0.3±0.0031	Mm.21855	Peptidoglycan recognition protein 1, mRNA (cDNA clone MGC:11430 IMAGE:3969014)
	0.3±0.0027	Mm.289431	Eukaryotic translation elongation factor 2, mRNA (cDNA clone MGC:6761 IMAGE:3600352)
	0.3±0.0026	Mm.288567	Hemoglobin, beta adult major chain, mRNA (cDNA clone MGC:40691 IMAGE:3988455)
	0.3±0.0034	Mm.347700	Histone 1, H2ae, mRNA (cDNA clone MGC:90847 IMAGE:5713252)
	0.3±0.0017	Mm.378975	Nerve growth factor, gamma (Ngfg), mRNA
	0.33±0.0041	Mm.196110	Hemoglobin alpha, adult chain 1 (Hba-a1), mRNA
	0.33±0.0022	Mm.293683	Envoplakin, mRNA (cDNA clone IMAGE:3985477)
	0.33±0.0027	Mm.54161	Dopamine receptor D1A (Drd1a), mRNA
	0.33±0.0034	Mm.383994	Keratin complex 2, basic, gene 6a (Krt2-6a), mRNA
	0.33±0.0031	Mm.35134	ATPase, Ca++ transporting, cardiac muscle, fast twitch 1, mRNA (cDNA clone MGC:28518 IMAGE:4191741)
	0.33±0.0038	Mm.358887	Androgen binding protein beta, mRNA (cDNA clone MGC:19070 IMAGE:4193111)
	0.34±0.0024	Mm.271275	Interferon stimulated gene 12 (Isg12)
	0.34±0.0029	Mm.280038	S100 calcium binding protein A11 (calizzarin) (S100a11), mRNA
	0.34±0.0035	Mm.383398	Adult male testis cDNA, RIKEN full-length enriched library, clone:1700022P22 product:hypothetical protein, full insert sequence
	0.34 0.0034	Mm.304354	Sycp3 like Y-linked (Sly), mRNA
	0.37±0.0041	Mm.133037	EGL nine homolog 3 (C. elegans) (Egln3), mRNA
	0.35±0.0013	Mm.686	Actin, alpha, cardiac (Actc1), mRNA
	0.35±0.0029	Mm.390	Cytotoxic T-lymphocyte-associated protein 4 (Ctla4), mRNA
	0.36±0.0033	Mm.379132	Brix domain containing 1, mRNA (cDNA clone MGC:35797 IMAGE:4009314)
	0.36±0.0031	Mm.99953	Chromobox homolog 8 (Drosophila Pc class), mRNA (cDNA clone MGC:25653 IMAGE:4456898)
	0.36±0.0032	Mm.378975	Nerve growth factor, gamma (Ngfg), mRNA
	0.36±0.0036	Mm.347936	Williams-Beuren syndrome critical region protein 22 (Wbscr22)
	0.36±0.0037	Mm.187847	Stefin A2 like 1 (Stfa2l1), mRNA
	0.36±0.0014	Mm.1239	Glial fibrillary acidic protein, mRNA (cDNA clone IMAGE:40045436)
	0.37±0.0035	Mm.372314	Heat shock protein 1B (Hspa1b), mRNA

	0.37±0.0037	Mm.377124	Eosinophil-associated, ribonuclease A family, member 14 (Ear14), mRNA
	0.38±0.0019	Mm.205190	Myeloid/lymphoid or mixed-lineage leukemia 5, mRNA (cDNA clone IMAGE:30605195)
	0.38±0.0024	Mm.378953	Kallikrein 11, mRNA (cDNA clone MGC:19030 IMAGE:4167568)
	0.38±0.0022	Mm.788	Lymphocyte antigen 6 complex, locus E, mRNA (cDNA clone IMAGE:5025954)
	0.38±0.0037	Mm.278701	Sterol regulatory element binding protein 1 (Srebp1)
	0.38±0.0041	Mm.37953	PREDICTED: desmoglein 1 alpha [Mus musculus], mRNA sequence
	0.38±0.0036	Mm.22742	FXYD domain-containing ion transport regulator 2, mRNA (cDNA clone MGC:25914 IMAGE:4222609)
	0.38±0.0029	Mm.208991	Iron responsive element binding protein 2 (Ireb2), mRNA
	0.39±0.0021	Mm.261491	Ras homolog gene family, member T1, mRNA (cDNA clone IMAGE:3601117)
	0.39±0.0045	Mm.195877	Zinc finger protein 106, mRNA (cDNA clone MGC:29071 IMAGE:4459713)
	0.39±0.0036	Mm.323365	PREDICTED: hypothetical protein LOC68469 [Mus musculus], mRNA sequence
	0.39±0.0025	Mm.262094	Unc-93 homolog B1 (C. elegans) (Unc93b1), mRNA
	0.39±0.0024	Mm.273277	Tripartite motif protein 29, mRNA (cDNA clone MGC:28195 IMAGE:3988926)
13-*cis*-retinoic acid			
	Increased		
	131.57±14.32	Mm.258170	Crystallin, gamma E (Cryge), mRNA
	73.64±7.66	Mm.275362	Crystallin, gamma F (Crygf), mRNA
	23.16±3.14	Mm.26904	Crystallin, gamma A, mRNA (cDNA clone MGC:66631 IMAGE:6824353)
	18.97±2.27	Mm.378900	Crystallin, gamma D (Crygd), mRNA
	14.89±2.07	Mm.298885	Crystallin, gamma C (Crygc), mRNA
	6.23±1.01	Mm.2128	S100 calcium binding protein A9 (calgranulin B), mRNA (cDNA clone MGC:41215 IMAGE:1332797)
	6.16±1.11	Mm.21567	S100 calcium binding protein A8 (calgranulin A) (S100a8), mRNA
	5.35±0.74	Mm.178246	Chromodomain helicase DNA binding protein 3, mRNA (cDNA clone MGC:40857 IMAGE:5369285)
	4.49±1.34	Mm.741	Fatty acid binding protein 5, epidermal, mRNA (cDNA clone MGC:5786 IMAGE:3490535)
	4.43±0.36	Mm.378899	Crystallin, beta B3, mRNA (cDNA clone MGC:25487 IMAGE:4501690)
	4.39±0.74	Mm.358667	Receptor (calcitonin) activity modifying protein 2 (Ramp2), mRNA
	4.39±0.47	Mm.311439	Heterogeneous nuclear ribonucleoprotein M (Hnrpm), mRNA

	4.36±0.34	Mm.205190	Myeloid/lymphoid or mixed-lineage leukemia 5, mRNA (cDNA clone IMAGE:30605195)
	4.21±0.41	Mm.19889	Keratin complex 1, acidic, gene 16 (Krt1-16), mRNA
	4.08±0.96	Mm.358643	Troponin T1, skeletal, slow (Tnnt1), mRNA
	4.07±0.39	Mm.220038	DEAD (Asp-Glu-Ala-Asp) box polypeptide 5, mRNA (cDNA clone IMAGE:3598655)
	Decreased		
	0.15±0.0071	Mm.288567	Hemoglobin, beta adult major chain, mRNA (cDNA clone MGC:40691 IMAGE:3988455)
	0.22±0.0045	Mm.45436	Lysozyme, mRNA (cDNA clone IMAGE:2655292)
	0.25±0.0024	Mm.270157	Melanoma antigen (Mela), mRNA
	0.34±0.0031	Mm.271275	Interferon stimulated gene 12 (Isg12)
	0.35±0.0065	Mm.372314	Heat shock protein 1B (Hspa1b), mRNA
	0.36±0.0022	Mm.248615	Lectin, galactose binding, soluble 3 (Lgals3), mRNA
	0.36±0.0012	Mm.350930	Similar to spermiogenesis specific transcript on the Y 2, mRNA (cDNA clone MGC:118215 IMAGE:30920635)
	0.36±0.0042	Mm.273277	Tripartite motif protein 29, mRNA (cDNA clone MGC:28195 IMAGE:3988926)
	0.37±0.0063	Mm.3815	Syndecan 4, mRNA (cDNA clone MGC:11456 IMAGE:3154160)
	0.37±0.0044	Mm.30181	PDZK1 interacting protein 1, mRNA (cDNA clone MGC:19227 IMAGE:4241868)
	0.38±0.0011	Mm.175661	Interferon induced transmembrane protein 1 (Ifitm1), mRNA
	0.38±0.0034	Mm.4646	Keratin complex 1, gene 13 (Krt1-13), mRNA
	0.38±0.0022	Mm.2344	Guanine nucleotide binding protein, beta 1, mRNA (cDNA clone MGC:11501 IMAGE:3964965)
	0.39±0.0061	Mm.280038	S100 calcium binding protein A11 (calizzarin) (S100a11), mRNA

[a]-the analysis was carried out as described in the Material and Methods.

Figure S1

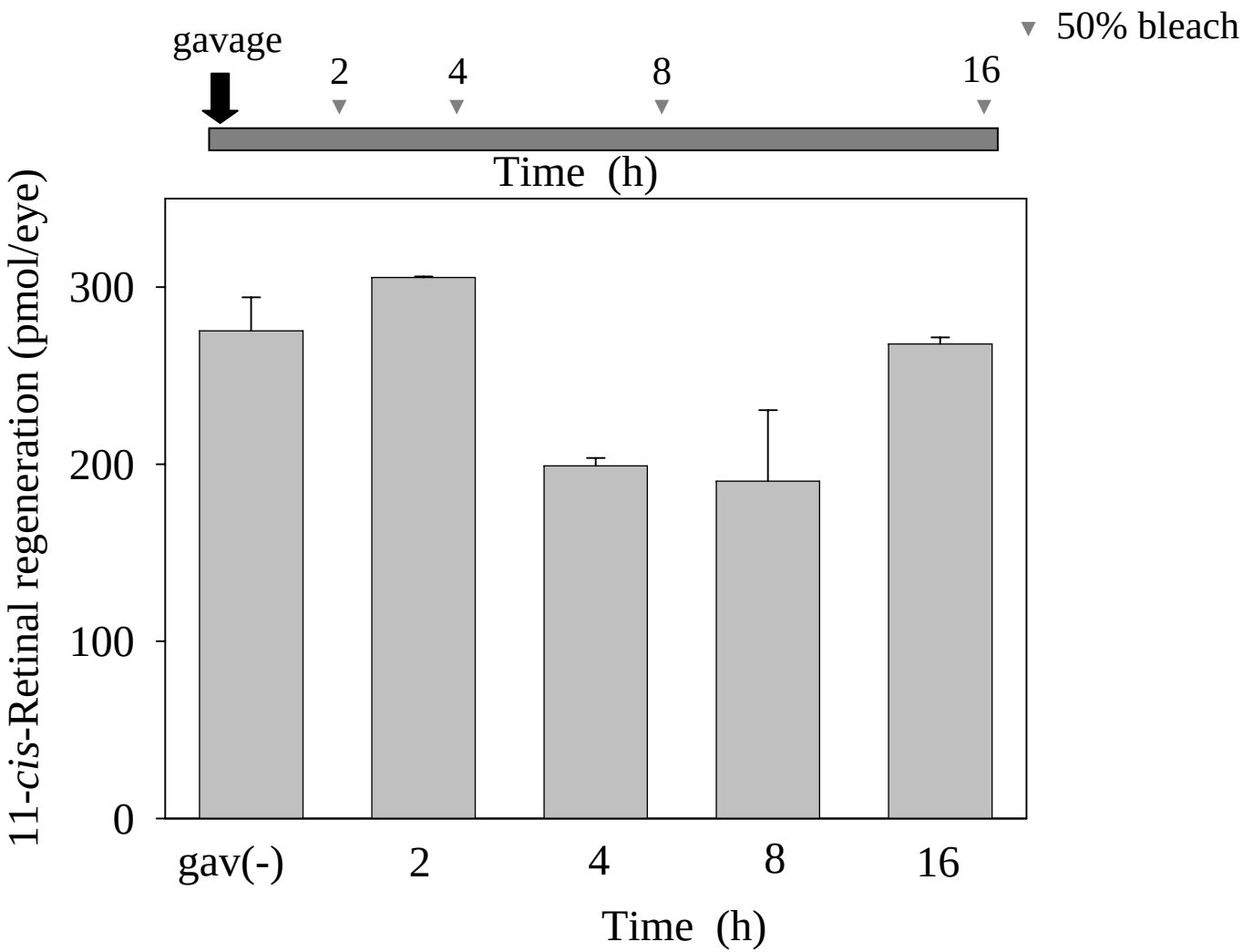
50% bleach
gavage
2
4
8
16
Time (h)
11-cis-Retinal regeneration (pmol/eye)
300
200
100
0
gav(-)
2
4
8
16
Time (h)

Figure S2

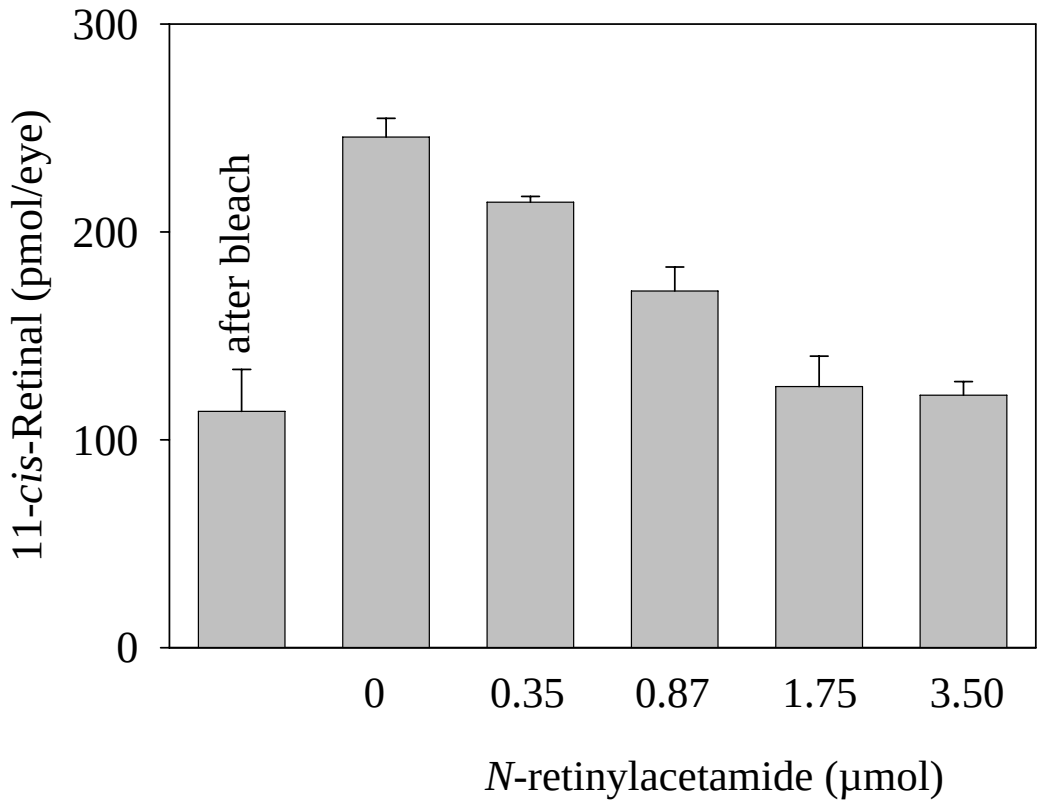
300
200
100
0
11-*cis*-Retinal (pmol/eye)
after bleach
0
0.35
0.87
1.75
3.50
N-retinylacetamide (µmol)

Figure S3

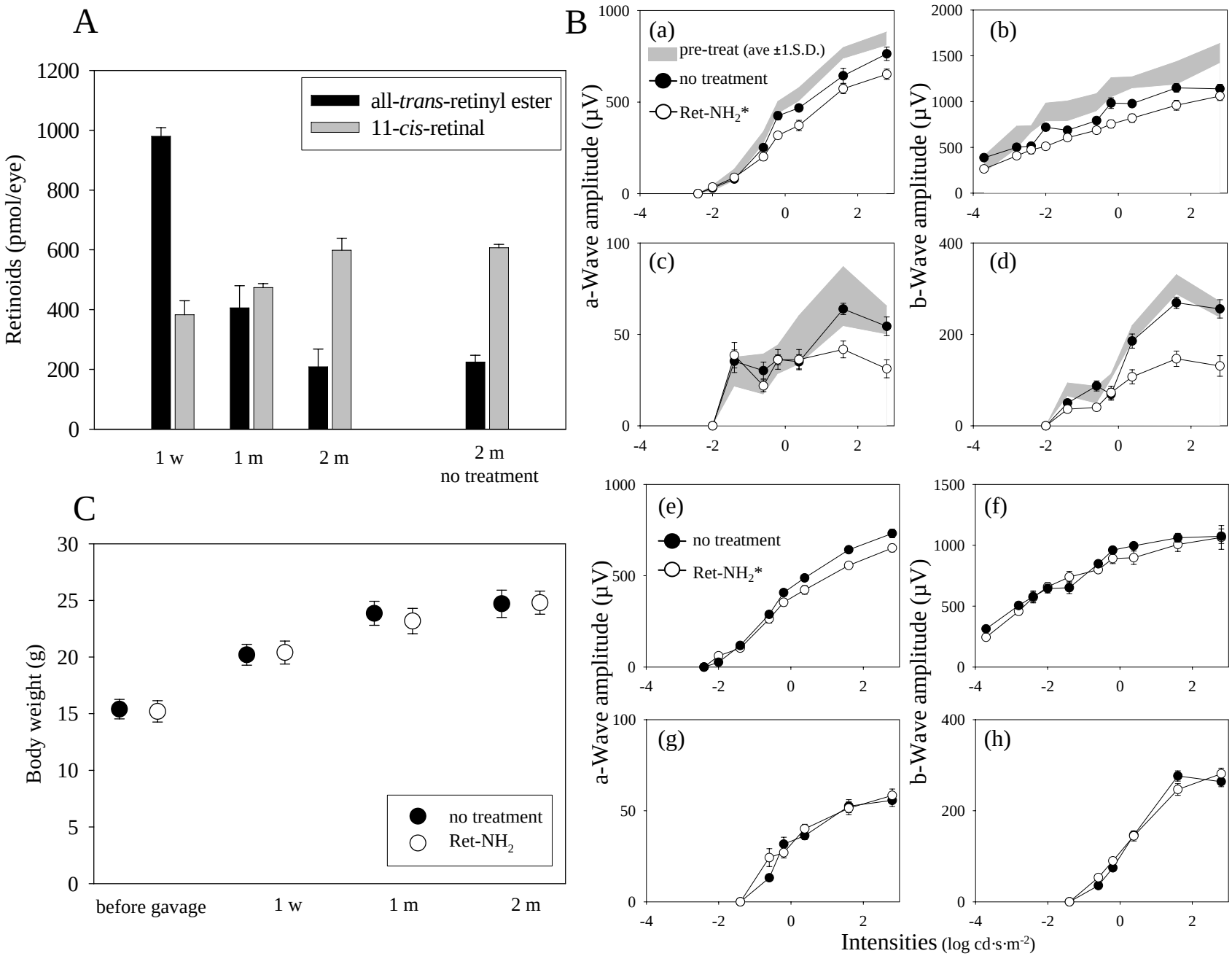

*, P<0.01 in (c) and (d)

Figure S4

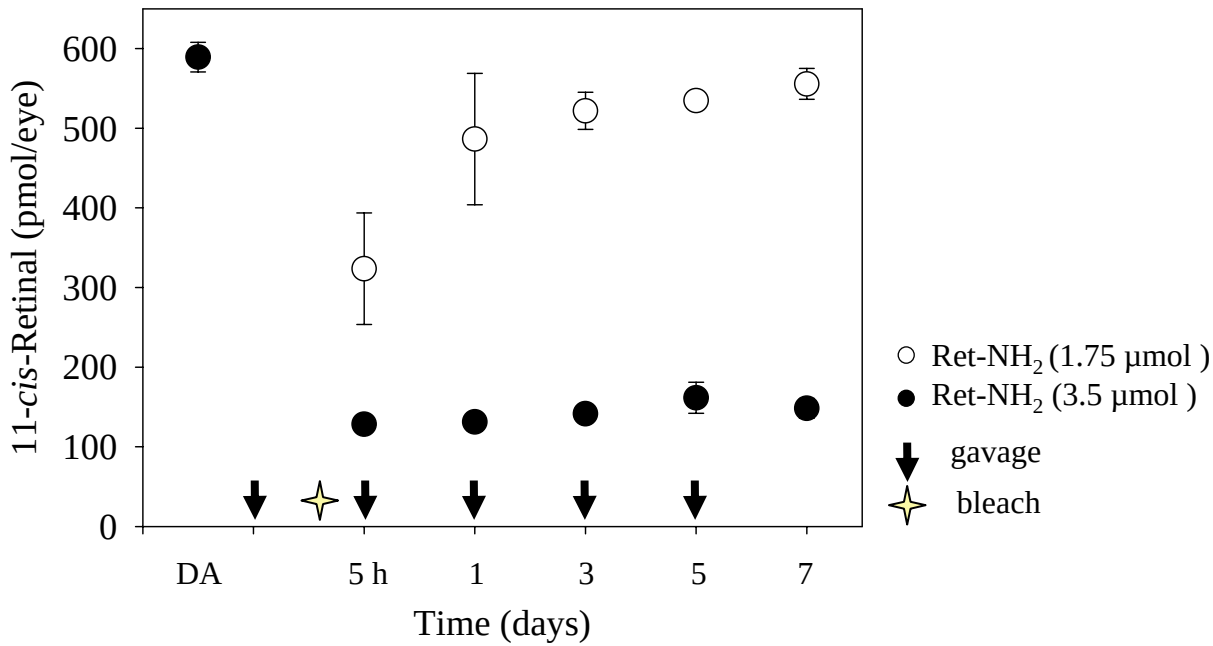
600
500
400
300
200
100
0
11-cis-Retinal (pmol/eye)
DA
5 h
1
3
5
7
Time (days)
Ret-NH2 (1.75 µmol)
Ret-NH2 (3.5 µmol)
gavage
bleach

Figure S5

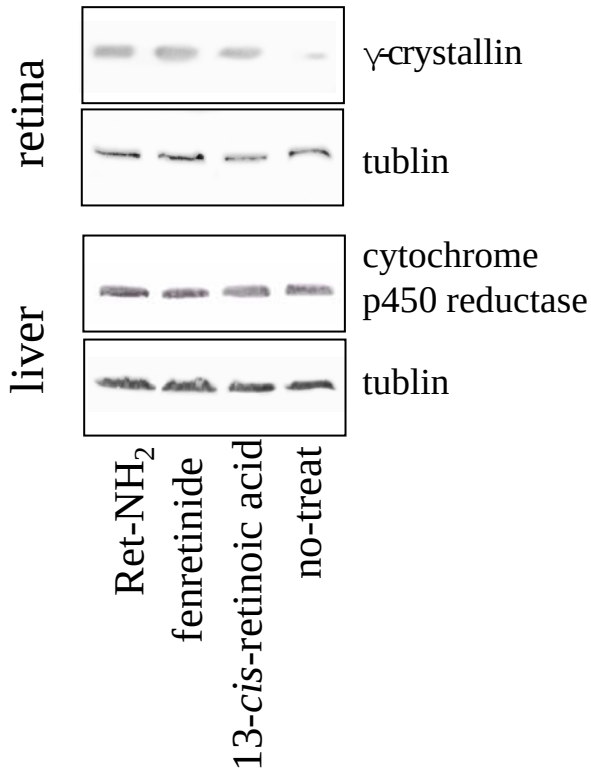
retina
liver
γ-crystallin
tublin
cytochrome
p450 reductase
tublin
Ret-NH2
fenretinide
13-cis-retinoic acid
no-treat